MONTHLY NOTICES

OF THE

ROYAL ASTRONOMICAL SOCIETY

Vol. 103 No. 5

MEETING OF 1943 SEPTEMBER 10

Professor E. A. Milne, President, in the Chair

The President announced the death of Professor Frank Schlesinger, an Associate of the Society, and paid the following tribute (the Fellows standing):—

"I regret to have to announce to the Society that Professor Frank Schlesinger, Associate of the Society, died on 1943 July 10, at the age of seventy-two. He had been an Associate since 1914, and he received the Gold Medal of the Society in 1927.

"He had been Director of the Allegheny Observatory from 1905 to 1920, and Director of the Yale Observatory from 1920 to 1941, when he retired from the Directorship. He was President of the International Astronomical Union from 1932 to 1935.

"He was distinguished for his precision work in astronomical photography, especially for his work on parallaxes and proper motion, in the measurement of which he attained previously unrealised accuracy and a previously unrealised wealth of results. He devoted much care and fertile ingenuity to the elimination of all possible errors in photographic parallax work, and in particular was responsible for the use of a rotating sector to reduce the brightness of the parallax star to that of the field stars.

"Schlesinger was known personally to many of the Fellows of this Society, both from his visits to this country and his Presidency of the I.A.U. His robust personality is held in affectionate remembrance. Yale has been the home of many famous scientists, and in Schlesinger we mourn one who worthily carried on that high standard."

The President announced that Professor Chapman, owing to pressure of other duties, had resigned from his position as Vice-President and from the Council. Council had elected Mr. F. J. Hargreaves as Vice-President, and the Astronomer Royal had accepted the vacant seat on the Council.

The election by the Council of the following Fellows was duly confirmed:—

Harold William Heaslip, 32 Orlando Street, Stratford, New Zealand;
Paul Ledoux, c/o Royal Astronomical Society, Burlington House, London, W. 1;
John Walter Ryde, F.Inst.P., Research Laboratories of the General Electric Co., Ltd., Wembley, Middlesex;
Karai Sivachidambara Mahesa Sarma, Pulavar House, Karainagar, Ceylon; and
Frank Sheldrake, B.Sc., 43 Victoria Road, Sheffield, 10.

The following candidates were proposed for election as Fellows of the Society, the names of the proposers from personal knowledge being appended:—

William Edward Beart, c/o B.B.C., Tatsfield, Westerham, Kent (proposed by J. G. Porter);

Miss Kathleen Maud Johnston, Acton Reynold Girls' School, near Shrewsbury (proposed by U. L. Johnstone);

Dennis Edwin Piper, 8 Kent Gardens, Ealing, London, W. 5 (proposed by H. Dingle);

Charles John Veale, 111 Holden Road, London, N. 12 (proposed by D. H. Sadler); and

Achill Wheatley, B.Econ., 42 Farm Avenue, London, N.W. 2 (proposed by G. Byfield).

Sixty-seven presents were announced as having been received since the last meeting.

Professor Rosseland delivered the George Darwin Lecture (see p. 233), taking as his subject "The Pulsation Theory of Cepheid Variables."

At the request of the lecturer, some discussion took place after the Lecture.

THE PULSATION THEORY OF CEPHEID VARIABLES

George Darwin Lecture, delivered by Professor Svein Rosseland, Assoc.R.A.S., on 1943 September 10

1. *Introduction.*—In the study of stellar motions it was natural that the translational motion of a star as a whole should be studied first, since it is easiest to measure, and because it obviously has an important bearing on the state and evolution of the galaxy as a whole.

The next step is to consider the *internal* motions of the stars, that is the motion relative to the centre of gravity. We then enter an interesting and as yet little explored field of astrophysics, the application of hydrodynamics to stellar problems. Historically it goes back to the work on the equilibrium of rotating fluid masses by mathematicians of the past century, among whom Sir George Darwin was one of the most eminent. This particular phase of the problem was brought to a preliminary close by the work of Sir James Jeans. Quite different aspects of the problem were opened up by the work of Sir Arthur Eddington on stellar constitution and the pulsation theory of variable stars some twenty-five years ago. It is on these studies that later work on stellar hydrodynamics has been based.

The simplest type of large-scale motion in a star is a rotation round a fixed axis, the angular velocity being variable or constant in space. Both from the point of view of theory as well as observation this problem must be said to be still in a preliminary stage.

A second type of possible large-scale motion is an expansion or contraction of the star as a whole. This type of motion may be said to be represented in the Sun by the outward motion in the corona. Similar motions probably take place in most stars, and are most conspicuous in Wolf-Rayet stars and novæ, where the expansion may be said to be observed directly. In Cepheids and other periodic variable stars it is believed, on the other hand, that a *periodic* type of expansion and contraction is at the root of the phenomena. It is reasonable to expect that radial pulsations play a considerable part also in semi-regular variable stars. But here some other type of motion is entering into competition with the simpler types of pulsation.

2. *Origin of the Pulsation Theory.*—The idea that stars may perform spherical pulsations originated in connection with the problem of interpreting the behaviour of Cepheid variables. The variability of δ Cephei was discovered by Goodricke * in 1783. The preceding year Goodricke had discovered the variability of β Persei, and rightly inferred from the form of the light-curve that it was produced by eclipses in a binary system. Knowing the frailty of the human mind one might have expected that Goodricke would have jumped to the conclusion that δ Cephei was just another eclipsing variable. But Goodricke reserved his judgment, and very wisely so.

The first suggestion that Cepheids might owe their light variation to a pulsation was made by the German physicist August Ritter †, who also developed the first rudiments of the pulsation theory. Ritter discovered that the slowest mode of pulsation of a homogeneous star has a period inversely proportional to the square root of the density. He also found that this mode of pulsation becomes unstable when the ratio of specific heats falls below 4/3, a result that holds generally for all gaseous stars. This, however, was long before anything was known of radial pulsations from direct observations and astronomers probably paid little attention to Ritter's suggestion. When, in 1894, Belopolsky ‡ discovered the periodic variation in the position of the lines in the spectrum of δ Cephei, this fact was not interpreted as a confirmation of the pulsation hypothesis, but as evidence that Cepheids were binary stars. It was twenty years before this

* *Phil. Trans. R.S.*, 75, 474, 1783. † *Wiedemanns Ann.*, 8, 172, 1879. ‡ *A.N.*, 136, 281, 1894.

belief was seriously questioned, although on the whole it was based on analogy only.

Plummer * was the first to throw doubt on the binary hypothesis of Cepheid variation, and Shapley † ruled it out by a careful analysis of observational facts, and suggested the pulsation hypothesis as an alternative.

Shapley's most convincing argument was that the size of the orbit of the hypothetical companion to a Cepheid appears to be too small to leave room for the principal star, so that the companion would have to move well inside the primary. This argument still stands, and those astronomers who have tried to retain some features of the binary hypothesis have therefore assumed a Cepheid to consist of two partially overlapping stars. This latter picture is, for instance, at the base of the recent interesting theory of Hoyle and Lyttleton ‡, which, however, is more akin to the ordinary pulsation theory than to the original binary hypothesis.

Shapley was well aware of the importance of the period-density relation demanded by theory. Incidentally, the same law holds also for other types of oscillations under gravity, as was shown by Lord Kelvin § for spheroidal oscillations of a homogeneous and incompressible star, and which led Moulton || to suggest that this type of oscillation might be realized in some variable stars.

The next paper on the pulsation hypothesis was a short and brilliant article by Eddington.¶ The following year Eddington ** published his famous papers on the Cepheid problem, which raised the pulsation hypothesis to the rank of a mathematical theory, where the discussion is concerned with quantitative issues.

At that time the principal observational facts about Cepheids were the *periods*, the general form of the *light-curve*, the *velocity-curve* and, finally, the period-luminosity relation, discovered by Miss Leavitt.††

Since that time more information about Cepheids has accumulated. More is now known about the correlation between period and mean density, so that a first check on the theoretical law can be made. Also much more material concerning the form of the light- and velocity-curves is available. In 1926 Hertzsprung ‡‡ announced the existence of a definite relation between the form of the light-curve and the length of the period. The existence of such a relation has been widely accepted, and this is also partly responsible for the sub-classification of Cepheids in the Robinson classes A, B, C and D. However, more recent work by Shapley §§ and his collaborators indicates that this tendency has been over-emphasized.

3. *Micro-Pulsations.*—Owing to mathematical difficulties, the problems of the pulsation theory must be approached in successive steps. The first step taken was to develop the theory within the framework of ordinary acoustics, where it is possible to work with wave motions which can be linearly superposed to form compound waves, assuming the oscillations to be adiabatic. In the next step anharmonic terms in the equations of motion are included and their modifying influence estimated. They represent the loss of wave energy by dissipation.

In the "acoustic" limit the pulsation problem is reduced to the study of a certain linear differential equation for the amplitude of pulsation. Since the star is an isolated structure in space, the solutions must satisfy the condition that pressure vanishes at the surface. Also the amplitude must be finite everywhere in the star. The solutions conforming to these requirements correspond to an infinite number of possible standing vibrations. The slowest vibration is called the fundamental mode, and is the one expected to be excited in pulsating variables.

* *M.N.*, 73, 665, 1913. † *Ap. J.*, 40, 448, 1914. ‡ *M.N.*, 103, 21, 1943.
§ *Phil. Trans. R.S.*, 153, 608, 1863. || *Ap. J.*, 29, 257, section iii, 1909.
¶ *Observatory*, 40, 290, 1917. ** *M.N.*, 79, 2, 177, 1918.
†† *H.C.*, No. 173, 1912. ‡‡ *B.A.N.*, 3, 115, 204, 1926.
§§ *Cf.* Shapley, McKibben and Mohr, *Proc. N.A.S.*, 26, No. 5, 326, 1940; Shapley and McKibben, *H.A.*, 90, No. 10, 1940.

The most immediate result of the pulsation theory in the acoustic limit is the period-density relation

$$P\sqrt{\rho} = K = \text{constant},$$

where P is the period and $\bar{\rho}$ is the mean density.

The value of K differs for different stellar models. It appears that for stars having the same ratio of specific heats, K will be largest for homogeneous stars, and will decrease as we pass on to stars in which the mass is more concentrated towards the centre. This was pointed out by Miller * for the case of polytropic stars, and further confirmed by the work of various authors.†

Using this theoretical formula as a basis for the analysis of the observations, it is convenient to use a diagram in which $\log P$ is plotted against $\log \sqrt{\rho}$. For stars of the same model the plot should then reduce to a straight line forming an angle of 45° with the axes.

In Fig. 1 such a diagram is given, the densities being obtained from data on the masses and radii of variable stars given in a recent paper by the Gaposchkins.‡

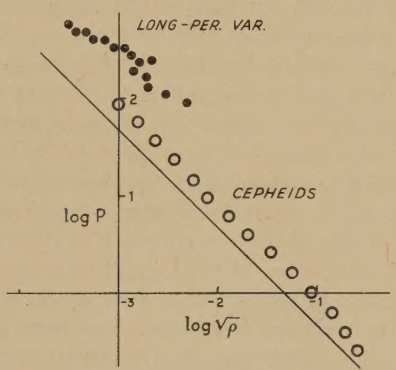

FIG. 1.—*Period-density relation for short-period variables and Cepheids (open circles) and long-period variables (filled circles).*

It appears that stars of the short-period and Cepheid types fall very closely along a straight line, inclined about 45° to the axes, in conformity with theoretical expectations. The same tendency is also quite plainly present for the long-period variables, but not nearly so clearly as for Cepheids. It is very remarkable, however, that these latter variables fall along a line which is different from that of the Cepheids. The data for semi-regular variables, as given by the Gaposchkins, would have fallen in the space between the Cepheid and long-period lines. At the short-period end of the Cepheids the empirical line shows a slight tendency to bend towards the left. This may be an indication that the stars here are a mixture of two types, one type falling along the straight Cepheid line and the other type falling along a parallel line to the left. That this is no mere guess is shown by the fact that Schwarzschild § found that the short-period variables in Messier 3 fall into two classes when plotted in a diagram roughly equivalent to a period-density diagram. If these stars were introduced in Fig. 1 one group would have fallen approximately along the extension of the short-period Cepheid row, while the other would have fallen to the left of this row. It is to be anticipated that a future representation of this diagram, based on accurate data, will show the stars as clustering around a system of lines running more or less parallel. This surmise is

* *M.N.*, **90**, 59, 1929.
† *Cf.* T. E. Sterne, *M.N.*, **97**, 582, 1937; P. Ledoux, *Astrophysica Norvegica*, **3**, 193, 1940.
‡ *Proc. American Phil. Soc.*, **86**, 329, 1943.
§ *H.C.*, No. 437, 1940.

confirmed by plotting the semi-regular variables, arranged according to physical similarity, in a period-density diagram. Each group is found to cluster along a separate line to the left of the long-period line. Owing to the uncertainty of the data it was not thought worth while to introduce these stars in the diagram at the present time.

The interpretation of these results is obviously beset with great difficulties. If all pulsating variables belong to the same stellar model, we should obviously expect them to fall along the same line in the diagram. According to present-day views on stellar structure, the mass distribution in the stars is not very different from that of the standard model, and the ratio of specific heats should not differ much from 5/3. The straight line in the diagram corresponds to this case. It is apparent that Cepheids and ordinary short-period variables fall well to the *right* of this line. The long-period stars fall widely off the line, still further to the right, while the only group of stars that conform to expectations is the small group of short-period variables in Messier 3, discovered by Schwarzschild.

One might suggest, as was done by Schwarzschild *, that some stars pulsate in higher modes. But this suggestion does not seem to be very helpful, seeing that the stars have a predominant tendency to fall to the right of the theoretical line, while overtone pulsations should appear to the left of the line. The suggestion would also raise a delicate problem, difficult to solve, as to why these stars do not show some trace of the fundamental mode, which is the one likely to be most easily excited.

Another suggestion would be to admit that different groups of stars have different values of the ratio of specific heats. A drop from 1·6 to 1·4 in γ would be sufficient to bring the theoretical line into coincidence with the observed Cepheid line. A much more drastic reduction would be necessary to interpret the data on long-period variables in this way. Thus far, however, there is no physical basis for such an assumption.

Another way to meet the observational requirements would be to assume that different groups of stars have different mass concentrations. To rectify the Cepheid line in this way it would be necessary to assume these stars to have a ratio of central to mean density of the order 10 : 1, whereas for the standard model this ratio is equal to 54 : 1. But even this drastic measure would not suffice to explain the position of the long-period variables in the diagram.

4. *Anharmonic Pulsations.*—Before drawing definite conclusions about the physical constitution of Cepheids on the basis of the period-density diagram, it is proper to discuss how far the results are influenced by the mathematical approximations involved in the theory. There is all the more reason for doing so since we know that the simple theory is widely off the mark for the velocity-curve and the light-curve. This being admitted, there is no *a priori* reason why this same approximation should predict the correct period.

That an improved theory is likely to predict longer periods is something we may infer on general grounds. Consider, for instance, the simple case of an ordinary pendulum. Infinitely small oscillations are sinusoidal, and the period is independent of the amplitude, just as in the case of small oscillations of a star. For increasing swing of the pendulum, however, the oscillations cease to be sinusoidal, and are instead represented by elliptic functions. At the same time the period increases. In fact the length of the period can be inferred from the change in shape of the curve giving velocity against time.

In a fairly general way we may expect the same situation to hold for the pulsations of a star. As the velocity-curve differs more and more from a simple sine curve, so the period may be expected to lengthen relative to the period computed from the elementary theory.

The first step towards an extended pulsation theory was made by Eddington †, its purpose being to prove that theory predicts a faster rise of the velocity to a maximum

* *H.C.*, No. 437, 1940. † *M.N.*, 79, 177, 1918.

than the subsequent drop to a minimum. A dependence of period on amplitude was not envisaged in this work, which later was extended by Miss Kluyver.*

To proceed further it is necessary to recast the theory in such a way as to avoid making implicit assumptions about the periods.† The natural procedure is then to express the displacement as an infinite series of elementary oscillation amplitudes, with undetermined time coefficients. When this series is introduced into the equation of motion it breaks up into an infinite number of ordinary differential equations for the time coefficients. If we include second-order terms only, these equations are of the same form as the equations for an infinite set of coupled linear oscillations, with the one difference that a self-coupling term occurs. This term, however, is likely to be the largest of the lot. The time coefficient of the oscillation may then be simply expressed by elliptic functions. Although we cannot expect this very simplified treatment to give a complete account of Cepheid pulsations, it is nevertheless entitled to some attention.

The form of the velocity-time curve thus obtained is determined by two constants only, one being the elementary period of oscillation, and the other the ratio of the pulsation amplitude to the radius of the star.

In Fig. 2 is drawn a typical example of such a velocity-time curve, in which the rise to a maximum is made to be about four times faster than the subsequent drop to

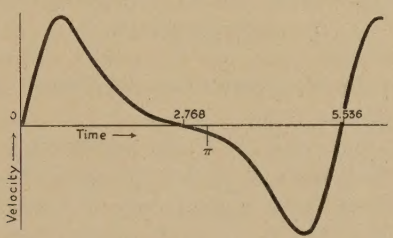

FIG. 2.

minimum velocity. If the pulsation had been harmonic, the period in this diagram should have been $\pi = 3{\cdot}14159\ldots$ It will be apparent, however, that for this particular curve the period is about 5·5, that is about 70 per cent. larger than the elementary period. A correction of this order would serve to make observation and theory agree for the Cepheids. However, it does not seem possible to attach much importance to this apparent agreement, as it seems to imply a far too large value of the amplitude. A calculation, based on the homogeneous model, leads to the result that the ratio of amplitude to radius should, in this case, be of the order 1/4, which is much larger than the observed values, which are of the order 1/12 or smaller. The inclusion of a few more coupling terms might make considerable difference to this result. To estimate the importance of such terms it would be desirable to perform rather extensive numerical integrations, which are best done on a differential analyser.

5. *Resonance Phenomena.*—About eight years ago Woltjer ‡ drew attention to some special features appearing in the problem of anharmonic pulsations when some of the elementary periods are nearly commensurable. Conditions are particularly simple if two modes having commensurable elementary periods are both excited. It was suggested by Miss Kluyver § that the peculiarities in the light-curve of RR Lyræ arise in this way. The light-curve of this star shows two distinct periods, of which the principal one is $0^d{\cdot}56685$ and the secondary one $38^d{\cdot}21$, which is 67·4 times longer than the principal period, suggesting a beat-frequency due to the fundamental mode being almost commensurable with some higher mode.

The position of this hypothesis might be strengthened if direct observations of

* *B.A.N.*, 7, 265, 1937.
† The details of these calculations are given in the Appendix.
‡ *M.N.*, 95, 260, 1935.
§ *B.A.N.*, 7, 313, 1936.

overtone pulsations were forthcoming. Thus far the only plausible instance seems to be the star δ Scuti, which according to Fath * shows three distinct periods:

$$P_0 = 0^d.193730; \qquad P_1 = 0.^d157382; \qquad P_2 = 0^d.095156.$$

Without stretching the figures too much, these may be interpreted as successive overtone pulsations. Schwarzschild † has suggested that the group of variables in M3 found by him to have anomalous positions in a period-density diagram might be performing overtone pulsations. As mentioned earlier this suggestion would seem to need further confirmation before being accepted.

6. *The Light-Curve.*—In a complete solution of the pulsation problem the light-curve could, of course, be predicted from a knowledge of the velocity-curve and the simultaneous variations in density and temperature. At the moment such a solution is not at hand. Still it is interesting to ask how far the light-curve may be predicted by using the observed velocity-curve, and making reasonable assumptions for the variations of temperature and density. An attempt along these lines was made by Schwarzschild.‡ To meet the observational fact that the luminosity is nearly in phase with the velocity and not the radius, Schwarzschild adopted for the photospheric density a semi-empirical expression containing a linear combination of velocity and radius, with constant, adjustable coefficients. This means that the density wave is *not* of the standing type but is a travelling wave. In this way Schwarzschild was able to obtain a close representation of the observed light-curve of δ Cephei. More recently Scott § made a corresponding analysis for the long-period variable *Mira*, using the radial velocity of the bright lines in the spectrum.

7. *Travelling Waves.*—This leads on to the outstanding problem of the Cepheids —the problem of phase retardation, or what is the same thing, the reason for the wave in the atmosphere of a Cepheid being of the nature of a travelling wave.

To produce a wave of this kind in a bounded system it is necessary that wave energy be somehow changed into heat, dissipated in other ways, or temporarily stored. Illustrative examples may be found in everyday experiences. An ocean wave breaking in over a sloping beach is so strongly dissipated that the reflected wave is too weak to change materially the travelling incident wave, whereas a wave reflected from a vertical wall is changed into an essentially standing wave. Another example is the temperature wave produced by the Sun in the ground. This wave is strongly damped by absorption, and shows a consequent slowing-up of the speed and a considerable phase retardation.

In a star the free boundary acts like a reflecting wall, and in the absence of dissipation a radial pulsation should be of the standing type of oscillation. The agencies able to dissipate wave energy in a star are viscosity and turbulence in the widest sense, including prominence and sunspot activity, and dissipation by conduction and radiation of heat.

That ordinary viscosity is unimportant here was proved by Persico ‖, while Eddington ¶ showed that the same holds for ordinary conduction and radiation phenomena. Two years ago, however, Eddington ** pointed out that the existence of the hydrogen convection zone in the stars may make a considerable difference to this problem. Preliminary calculations indicate that a quantitative agreement between theory and observation on this basis is possible. More detailed calculations of this problem, taking into account the second-order modifications in the equations of motion, would seem to be of considerable interest.

8. *Conclusions.*—The main impression given by the pulsation theory in its present stage is one of incompleteness. While it is true that some features of the theory have been pretty exhaustively discussed in the acoustic limit, this is a very unsatisfactory representation of observed facts, and must be replaced by the theory of anharmonic

* *L.O.B.*, 19, 77, 1940. † *H.C.*, No. 437, 1940. ‡ *H.C.*, No. 429, 1938.
§ *Ap. J.*, 95, 58, 1942. ‖ *M.N.*, 86, 98, 1925. ¶ *M.N.*, 87, 539, 1927.
** *M.N.*, 101, 182, 1941; 102, 154, 1942.

pulsations, which is still in its infancy. But it is only within such a framework that the pulsation theory can account for the variation in form of the velocity-curves, and also for the quantitative details of the period-density diagram.

The separation of Cepheids, long-period variables and the M_3 group in the diagram appears to form an outstanding problem, which has not so far received sufficient attention. Inherent physical differences between the stars of these groups seem to be suggested.

As regards the phase retardation of luminosity, the pulsation theory has little to say at present, but Eddington's suggestion about the hydrogen convection zone may lead to a solution of the problem. Further work on anharmonic pulsations may be of considerable importance in this connection. This also holds for the interpretation of the period-luminosity law, which has received little attention so far. Inasmuch as this law provides a relation between the density and mass of a Cepheid, it gives a criterion for the initiation of the pulsations * during the evolution of a star.

On the whole, the pulsation theory seems to have survived nearly thirty years of hard tests without having come up against insurmountable difficulties. This would seem to indicate that its basic assumptions are sound, and that it will remain a fruitful field of work in the future development of astrophysics.

APPENDIX

The Theory of Anharmonic Pulsations

1. *The Canonical Equations.*—Consider the adiabatic pulsations of a spherical, non-rotating star. Let r, p, ρ and g denote radius vector, pressure, density and gravity of an individual particle in the Lagrangian sense, and let a, p_0, ρ_0 and g_0 denote these quantities at a given initial time t_0. The equation of motion is

$$\ddot{r} = -\frac{1}{\rho}\frac{\partial p}{\partial r} - g. \tag{1}$$

We want to transform this equation to bring out the fact that the star may oscillate in different modes, with separate frequencies. For this purpose we recall that for oscillations of infinitely small amplitude the displacement of an individual particle may be written into the general form

$$r - a = \sum_k \xi_k \cos(\sigma_k t + \epsilon_k), \tag{2}$$

where ξ_k form an infinite set of functions depending on a, which are finite all through the star, $\sigma_k/2\pi$ is the frequency of oscillation corresponding to the amplitude ξ_k, while the ϵ_k's are arbitrary phase constants. The amplitudes ξ_k are orthogonal to each other in the sense that they satisfy the relation

$$(\sigma_i - \sigma_k)\int_0^M \xi_i \xi_k dm = 0, \tag{3}$$

M denoting the total mass of the star, of which dm is a mass element. The integral in (3) must thus vanish in all cases when σ_i differs from σ_k, which in practice means that the two modes involved are different.

Suppose now that we assume the displacement written in the form of an infinite series

$$r - a = \sum_k \xi_k q_k(t), \tag{4}$$

where q_k depends on time only, and degenerates into a simple cosine as the amplitude

* *Cf.* Eddington, *M.N.*, 102, 154, 1942.

becomes infinitely small. The quantities q_k may be considered as generalized coordinates of the state of oscillation of the star. The corresponding Hamiltonian momenta are given by

$$p_k = \frac{\partial}{\partial \dot{q}_k} \int_0^M \tfrac{1}{2}\dot{r}^2 dm = I_k \dot{q}_k, \tag{5}$$

where

$$I_k = \int_0^M \xi_k^2 dm, \tag{6}$$

since the integrals over all cross products of different amplitudes vanish in virtue of (3).

Let us next transform equation (1) term by term. To do this we introduce the expression (4) for r, multiply the equation by $\xi_k dm$ and integrate over the star. The left-hand side then becomes equal to $\dot{p}_k$.

In order to transform the first term on the right-hand side we write it in the equivalent form

$$\frac{1}{\rho}\frac{\partial p}{\partial r} = \frac{1}{\rho}\frac{\partial a}{\partial r}\cdot\frac{\partial p}{\partial a} = \frac{r^2}{\rho_0 a^2}\frac{\partial p}{\partial a}, \tag{7}$$

in virtue of the equation of continuity, which in the present case assumes the form

$$dm = 4\pi\rho r^2 dr = 4\pi\rho_0 a^2 da = \text{const., in time.} \tag{8}$$

Since $\xi_k = \partial r/\partial q_k$ it follows that, on performing a partial integration,

$$\int_0^M \frac{1}{\rho}\frac{\partial p}{\partial r}\xi_k dm = 4\pi\int_0^R r^2\frac{\partial r}{\partial q_k}\cdot\frac{\partial p}{\partial a}da = -4\pi\int_0^R p\frac{\partial}{\partial q_k}\left(r^2\frac{\partial r}{\partial a}\right)da, \tag{9}$$

where R denotes the radius of the star. Assuming the adiabatic relation

$$p = p_0(\rho/\rho_0)^\gamma \tag{10}$$

to hold, and using (8), the right-hand side of (9) assumes the final form

$$\frac{\partial}{\partial q_k}\int_0^M \frac{1}{\gamma-1}\frac{p}{\rho}dm = \frac{\partial U}{\partial q_k}, \tag{11}$$

where U is now the total thermal energy of the star.

Let us finally turn to the transformation of the second term on the right-hand side of equation (1). Since $g = g_0 a^2/r^2$, we find that

$$\int_0^M g\xi_k dm = \int_0^M g_0\frac{a^2}{r^2}\frac{\partial r}{\partial q_k}dm = -\frac{\partial}{\partial q_k}\int_0^M g_0\frac{a^2}{r}dm = \frac{\partial V}{\partial q_k}, \tag{12}$$

where V is the total gravitational energy of the star. Writing H for the total energy of the star, we have

$$H = \int_0^M\left(\tfrac{1}{2}\dot{r}^2 + \frac{1}{\gamma-1}\frac{p}{\rho} - g_0\frac{a^2}{r}\right)dm, \tag{13}$$

and the equations of motion assume the Hamiltonian form

$$\dot{p}_k = -\frac{\partial H}{\partial q_k}; \qquad \dot{q}_k = \frac{\partial H}{\partial p_k}; \qquad k = 1, 2, \ldots \textit{ad inf.} \tag{14}$$

2. *The Second-Order Approximation.*—The equations derived in the preceding section are quite general for spherical adiabatic pulsations. In the following, however, we shall be particularly concerned with the case when the third and higher orders in the displacement are neglected. While this approximation may also break down in

certain applications, it is nevertheless a useful step, as it indicates the direction in which the theory is to be amended.

Suppose that the Hamiltonian of the problem is expanded in powers of the co-ordinates q_k, and let H_1, H_2 and H_3 denote the terms of the first, second and third order respectively. The first-order term in the Hamiltonian will be zero, owing to the fact that the oscillations take place around a state of equilibrium. The second term, H_2, will contain that part of the energy which is taken into account in the linear approximation, while H_3 will represent the second-order correction.

We should, in general, expect H_2 to be of the form

$$H_2 = \sum_{ik} K_{ik} q_i q_k,$$

but owing to the fact that our basic functions ξ_k are orthogonal solutions of the first-order problem, the expression of H_2 is a sum of squares, and may be written as

$$H_2 = \sum_{k} \tfrac{1}{2} \sigma_k^2 I_k q_k^2, \tag{15}$$

where $\sigma_k/2\pi$ is the frequency of the kth proper vibration in the linear approximation.

There are no such limitations to the form of H_3, and we may write

$$H_3 = -\sum_{iks} C_{ik}{}^s \cdot q_i q_k q_s, \tag{16}$$

where the coefficients $C_{ik}{}^s$ are constants to be computed from the given stellar model.

The first row of Hamiltonian equations (14) then assume the form

$$\ddot{q}_s = -\sigma_s^2 q_s + (I_s)^{-1} \sum_{ik} C_{ik}{}^s q_i q_k; \qquad s = 1, 2 \ldots \tag{17}$$

This set of equations is formally identical with that of an infinite assembly of coupled linear oscillators.

3. *A Single Excited Mode.*—Of course it is not possible to solve equations (17) in full generality. In order to get an insight into the nature of the solutions we must consider special cases.

The simplest possible case which has any interest at all would seem to be one in which the displacement is given approximately by two terms only, say

$$r - a = q_1 \xi_1 + q_2 \xi_2. \tag{18}$$

We may suppose that ξ_1 is the amplitude of the excited mode of the star, which we may as well assume to be the fundamental mode, while ξ_2 is the amplitude of a higher mode, suitably chosen. This means that we approximate to the second-order term in the displacement by a linear combination of ξ_1 and ξ_2. A comparison of Miss Kluyver's computations of second-order corrections with Schwarzschild's curve for the second overtone oscillation suggests that such an approximation is not unreasonable when dealing with a star pulsating in the fundamental mode.

Retaining only the largest correcting term of the second order, the equation for q_1 assumes the form

$$\ddot{q}_1 + \sigma_1^2 q_1 = D q_1^2. \tag{19}$$

This equation is soluble in terms of elliptic functions. To bring the equation into the standard form we multiply by $\dot{q}_1$ and integrate once, which gives

$$\dot{q}_1^2 = C - \sigma_1^2 q_1^2 + \tfrac{2}{3} D q_1^3, \tag{20}$$

C being a constant of integration. It is now convenient to replace the coefficients C, σ_1^2 and D by the three roots of the equation

$$C - \sigma_1^2 q_1^2 + \tfrac{2}{3} D q_1^3 = 0. \tag{21}$$

These roots we denote by e_1, e_2 and e_3, and assume them to satisfy the inequalities $e_1 < e_2 < e_3$. Equation (20) then assumes the form

$$\dot{q}_1^2 = \tfrac{2}{3}D(q_1 - e_1)(q_1 - e_2)(q_1 - e_3). \tag{22}$$

In the next step we perform the transformation

$$q_1 = e_1 + (e_2 - e_1)\sin^2\phi, \tag{23}$$

$$\sigma_1 t = \sqrt{\frac{e_1 + e_2 + e_3}{e_3 - e_1}} \cdot 2u = 2\lambda u \tag{24}$$

and

$$k^2 = (e_2 - e_1)/(e_3 - e_1). \tag{25}$$

By this transformation equation (22) assumes the form

$$\left(\frac{d\phi}{du}\right)^2 = 1 - k^2\sin^2\phi, \tag{26}$$

which on integrating gives

$$u = \int \frac{d\phi}{\sqrt{1 - k^2\sin^2\phi}}. \tag{27}$$

By (23), q_1 will oscillate between e_1 and e_2 with a period π in the co-ordinate ϕ. To find the corresponding period in the time, we first find the period in u by tables of elliptic integrals, and next compute the time period from u by equation (24).

Leaving aside the term in q_2 for the moment, we may study the case when q_1 alone is important. The oscillations are then the same as for an infinitely small oscillation, except that the cosine has been replaced by a certain elliptic function. The observations deal chiefly with the velocity of pulsation, which in this case is proportional to $\dot{q}_1$. By (23), (24) and (26) we may express $\dot{q}_1$ as a function of the auxiliary angle as follows:—

$$\dot{q}_1 = \frac{\sigma_1(e_2 - e_1)}{2\lambda}\sin 2\phi \,.\, \sqrt{(1 - k^2\sin^2\phi)}. \tag{28}$$

For further progress we must fix the various arbitrary constants involved in the equations. We may do this, for instance, by saying that ξ_1 is the actual amplitude of pulsation of the star, *i.e.* the maximum positive extension in a radial direction of the given particle. This means that the maximum positive value of q_1 must be unity, which by (23) means that $e_2 = 1$. The two remaining roots consequently satisfy the equations

$$e_1 + 1 + e_3 = 3\sigma_1^2/2D, \qquad e_1 + e_3 + e_1e_3 = 0,$$

the solution of which is

$$e_3,\ e_1 = \tfrac{1}{2}E \pm \sqrt{(\tfrac{1}{4}E^2 + E)}, \tag{29}$$

where

$$E = 3\sigma_1^2/2D - 1.$$

A numerical test now shows that λ differs very little from unity in the region of admissible values of E, say from $E = 1$ to $E = \infty$. We may thus assume $\lambda = 1$ for general considerations.

When plotting curves of $\dot{q}_1$ as a function of u, for various values of E, it is found that to obtain any considerable skewness of the curve it is necessary that D is close to σ_1^2. This fact makes it possible to subject the theory to a quantitative test.

4. *The Case of a Homogeneous Star.*—In the general case it is very laborious to derive the coefficient D for a given stellar model, but in the simple case of a homogeneous

star, pulsating in the fundamental mode, it is relatively simple. We may then write

$$r/a = 1 + q\eta, \tag{30}$$

where

$$\eta = \xi/a = \text{constant}. \tag{31}$$

Recalling further that for a homogeneous star

$$p_0 = \tfrac{1}{2}\rho_0 \frac{GM}{R}\left(1 - \frac{a^2}{R^2}\right) \tag{32}$$

and

$$g_0 = GMa/R^3, \tag{33}$$

the Hamiltonian of the problem may be written in the form

$$H = \tfrac{1}{2}\dot{q}^2\eta^2\int_0^M a^2 dm + \frac{GM}{2(\gamma-1)R}\left(\frac{\rho}{\rho_0}\right)^\gamma \int_0^M \left(1 - \frac{a^2}{R^2}\right) dm - \frac{GMa}{R^2 r}\int_0^M a^2 dm. \tag{34}$$

For a homogeneous star

$$\int_0^M a^2 dm = \tfrac{3}{5}MR^2,$$

which leads to the following form for the Hamiltonian:—

$$H = \tfrac{3}{5}MR^2\left[\tfrac{1}{2}\eta^2\dot{q}^2 + GMR^{-3}\left\{\frac{(\rho/\rho_0)^\gamma}{3(\gamma-1)} - \frac{a}{r}\right\}\right]. \tag{35}$$

Expanding to the third power of η we get, after some calculations,

$$H = \tfrac{3}{5}MR^2\eta^2\{\tfrac{1}{2}\dot{q}^2 + \tfrac{1}{2}\sigma_1^2 q^2 - \tfrac{1}{2}\sigma_1^2(\gamma + \tfrac{1}{3})\eta q^3\}, \tag{36}$$

where

$$\sigma_1 = \sqrt{(3\gamma - 4)GM/R^3}$$

and is 2π times the frequency of the fundamental mode. The corresponding canonical equation of motion is

$$\ddot{q} + \sigma_1^2 q = \tfrac{1}{2}(3\gamma + 1)\sigma_1^2\eta q^2, \tag{37}$$

which means that

$$D/\sigma_1^2 = \eta(3\gamma + 1)/2. \tag{38}$$

For the monatomic value of γ ($\gamma = 5/3$), this gives $D/\sigma_1^2 = 3\eta$. The limiting value of η for $D/\sigma_1^2 = 1$ is thus $\eta = 1/3$, which means that the displacement ξ has the value $R/3$ at the surface of the star. The semi-amplitude of the oscillation being

$$K = \tfrac{1}{2}(e_2 - e_1)\xi, \tag{39}$$

and e_2 and e_1 being, in the limits considered, equal to 1 and $-\tfrac{1}{2}$ respectively, we find

$$K = \tfrac{1}{4}R \tag{40}$$

as the limit for the semi-amplitude. This value is 4 to 5 times larger than the value found for most Cepheids. There is therefore a considerable discrepancy to bridge over in some way. It appears unlikely that this might be done by varying the model, as the Roche model (a point mass at the centre surrounded by a mass less atmosphere) gives nearly the same result. In order to obtain a quantitative representation of the observed velocity curves on this general theoretical basis, it is thus necessary to extend the calculations to include more terms.

SOLAR FLARES AND MAGNETIC STORMS

H. W. Newton

(Communicated by the Astronomer Royal)

(Received 1943 August 13)

Summary

Data on specially intense solar flares from spectroscopic records (including recent spectrohelioscope observations) have been discussed in connection with the occurrence of magnetic storms. Certain features, including their great area and possible characteristics of spectrum, distinguish these very intense flares when they occur. Future observations should aim at including quantitative data to serve as an index of intensity. A geophysical measure of intensity should also be explored.

Far more often than could occur by chance, an intense flare is followed about a day later by a great magnetic storm, provided that the flare is not farther than about 45° from the centre of the disk. Assuming that a corpuscular stream is newly ejected at the time and place of an intense solar flare, the mean effective time of travel of the stream from Sun to Earth is about 26 hours, the most intense magnetic storms giving a shorter travel-time of about 20 hours. The distribution on the Sun's disk of flares preceding great magnetic storms is examined and suggests certain features of the corpuscular streams involved.

1. *Introduction*

In 1937 a paper * from Greenwich was presented to the Society giving evidence of a relationship (found independently by other workers) between bright chromospheric eruptions or flares and sudden synchronous disturbances in the ionosphere producing fade-outs. Associated with fade-outs are small synchronous perturbations in the Earth's magnetic field over the sunlit hemisphere.† Although these dual geophysical phenomena enter incidentally, the present purpose is to investigate the occurrence of large magnetic disturbances (magnetic storms) not synchronous with the solar flares, but following, as it is found, about 24 hours later.

In the third of four papers on the spectrohelioscope, the late Dr. G. E. Hale assembled data ‡ of unusually bright and extensive eruptions gleaned from spectroheliogram records between 1892 and 1930, and in addition the first observations of flares made with the newly invented spectrohelioscope in 1926. These exceptional solar outbursts, Hale stated, have mostly been followed by brilliant auroræ and widespread magnetic storms, and "the evidence seems to favour the view that the observed solar eruptions are directly connected with these terrestrial phenomena." A valuable feature of Hale's paper is the series of reproductions from spectroheliograms, which give a pictorial standard of comparison for later observers. Since Hale's paper in 1931, nearly a whole 11-year cycle of observations of solar flares has been co-ordinated and published under the auspices of the I.A.U. A simple statistical discussion of all the available data on intense flares is given in the present paper.§

* *M.N.*, **97**, 594, 1937.

† *Geomagnetism*, by Chapman and Bartels, **1**, 341, 1940.

‡ Hale, *Ap. J.*, **73**, 379, 1931. Another list was published independently just before by the present writer, *M.N.*, **90**, 824, 1930.

§ A short preliminary discussion appeared in *The Observatory*, **62**, 318, 1939.

2. *Observational Data*

(a) *Solar Data.*—The *Quarterly Bulletin on Solar Activity*, published from Zürich under the auspices of the I.A.U., contains data of every solar flare observed by international co-operation since 1934, *i.e.* from the beginning of the present 11-year solar cycle. The intensity of each flare is given as estimated by the respective observers on a qualitative scale of 1, 2, 3, the last being the most intense. Amongst the flares of intensity 3, a very few stand out as being comparable with the great eruptions listed by Hale. The selection of these super flares (designated herein as 3+) during the present cycle has been based on the replies to a questionnaire sent from Greenwich in 1939 to the observatories of Meudon, Mount Wilson and Zürich. To their selection has been added that from observations made in this country. Since 1939, the selection has depended on any available published notes and on the observations made at Greenwich and by Mr. M. A. Ellison at Sherborne. During the present cycle there were 14 flares of intensity 3+. Because of the special interest attaching to these intense flares, it is desirable that in future they should be designated in the *Solar Bulletin* together with any available measures of area and light intensity. Owing to their infrequency, the collecting of modern data will be slow, and therefore to those of the present cycle have been added the scattered records of great flares observed prior to 1934, drawn from the following sources:—

(1) Hale's list in *Ap. J.*, **73**, 379, 1931. (2) An independent list given in *M.N.*, **90**, 824, 1930. (3) A list of unusually bright *Hα* reversals seen on the disk, collected from various records between 1869 and 1882, given in *J.B.A.A.*, **50**, 273, 1940.

As regards (3), though a detailed comparison remains to be undertaken, there seems no doubt that brilliant *Hα* reversals seen on the disk are essentially the same phenomenon as the brilliant flares whose form is delineated by the spectroheliograph or the spectrohelioscope. In some cases considered in this paper ¶, the brilliant reversals of *Hα* and other lines were observed visually at the position where spectroheliograms recorded a brilliant flare. In compiling Table I from the above sources, three flares (1869 April 13, 1928 January 26 and September 14) have been relegated to the next intensity class (=3) to be discussed later.

To the above data has been added the unique observation made by Carrington and Hodgson of a pair of brilliant patches seen in integrated light over a giant sunspot on 1859 September 1 (see later note on spectrum).

(b) *Magnetic Data.*—A list of magnetic storms observed at Greenwich from 1875 to 1927 is given in the *Greenwich Photoheliographic Results*, 1927. This list has been continued annually in *The Observatory*. Previous to 1875, there is a list of storms recorded at Greenwich, 1848 to 1881, given by Maunder (from Ellis's original list) in *M.N.*, **65**, 538, 1905.

The lower limits of disturbance adopted in various discussions at Greenwich for a magnetic storm are 30′ in D or 150 γ in H or in V. For a "great" storm the corresponding lower limits are 60′ in D or 300 γ in H or in V. When a disturbance has a range in D of 90′ or 500 γ in H or in V, the storm is designated "very great". The great storms recorded at Greenwich are almost certainly world-wide, and the majority of them have a characteristic sudden start. With respect to this paper, two additions to the published list of small storms should be noted, viz. no. 25* 1882 November 21–22 (greatest range in $D=42'$) and no. 243* 1916 June 30–July 1 (greatest range in $H=174\ \gamma$).

(*c*) *Table of Data.*—Table I lists 37 solar flares of intensity 3+. In each of three cases (nos. 5, 15, 18), two flares have both been given half weight (owing to insufficient data) and are bracketed together. Of the 37 flares listed, 14 were observed in the present 11-year cycle and 23 over the seven preceding cycles.

¶ Table I: no. 8 (Hale); no. 11 (Fowler and W. J. S. Lockyer); no. 12 (Evershed); no. 19 (Hale) and no. 21 (Royds).

TABLE

Intense Solar Flares (Intensity 3+) within Sunspot

Ref. No.	Solar Flare					
	Date (1)	Time, U.T. (2)	Duration (3)	Area (4)	Longitude from C.M. (5)	From Centre of Disk (r/R) (6)
		h	h		°	
1	1859 Sept. 1	**11·3**	0·1	~ 100	12 W.	0·31
2	1869 Apr. 21	7 and 14	...	...	85 W.	·99
3	1870 Sept. 28	21	...	~1500	46 W.	·70
4	1872 Aug. 5	14	...	~ 300	72 E.	·94
5	1882 Nov. 18	11	2·0	< 500	5 E.	·31
	1882 Nov. 20	11	2·0	~ 500	21 W.	·45
6	1882 Nov. 21	12	...	~1500	34 W.	·62
7	1892 July 11	11·7	2·0	~ 500	32 E.	·71
8	1892 July 15	**17·0**	2·0	1500	22 W.	·65
9	1908 Sept. 10	5·6	< 4·0	2800	18 W.	·36
10	1909 May 12	14·6	...	1500	16 E.	·32
11	1909 Sept. 24	10	2·5	1500	8 W.	·23
12	1909 Sept. 28	**4·5**	> 1·0	> 1000	60 W.	·88
13	1916 June 29	9	1·0	1200	5 W.	·17
14	1916 Nov. 10	15·7	...	1600	18 E.	·45
15	1917 Feb. 7	16·0	...	2300	24 E.	·43
	1917 Feb. 8	15·7	...	550	11 E.	·25
16	1917 Feb. 14	16·1	...	2800	44 E.	·72
17	1917 Feb. 16	15·9	...	4800	20 E.	·44
18	1917 Aug. 8	14·4	...	1700	20 E.	·37
	1917 Aug. 9	14·6	...	4000	7 E.	·20
19	1926 Jan. 24	19·7	> 0·3	11,000	4 W.	·44
20	1926 Jan. 25	20	> 2·0	10,000	17 W.	·51
21	1926 Feb. 22	2·3	> 7·2	2900	10 W.	·52
22	1926 Oct. 13	13·2	1·5	4700	3 E.	·19
23	1930 Aug. 12	11	> 3·0	400	3 W.	·22
24	1936 Apr. 8	**16·8**	1·7	2500	8 W.	·48
25	1936 Dec. 30	10·9	> 1·7	1500	56 W.	·86
26	1937 July 16	**22·8**	1·5	...	21 W.	·47
27	1937 July 31	16·7	> 1·6	5000	67 E.	·91
28	1937 Sept. 30	10·2	1·0	3500	52 E.	·78
29	1938 Jan. 20	18·3	> 3·1	...	30 W.	·59
30	1938 Apr. 13	**9·5**	> 2·3	2000	10 E.	·53
31	1938 Apr. 15	8·5	> 1·3	1800	12 W.	·57
32	1938 Sept. 23	16·9	0·9	...	60 E.	·88
33	1938 Dec. 7	**18·2**	1·1	...	10 W.	·22
34	1939 Apr. 21	**16·5**	> 1·5	4500	59 E.	·88
35	1939 May 4	**9·5**	2·3	800	11 E.	·33
36	1941 Sept. 17	8·6	> 1·3	500	9 W.	·16
37	1942 Feb. 28	12·7	> 2·7	2200	3 E.	·22

I

Groups, and the Associated Magnetic Storms (1859–1942)

Ref. No.	Associated Sunspot				Magnetic Storm within ±2·0 Days			Source Reference
	C.M.P. U.T. (7)	Latitude (8)	Area (9)	Type (10)	Magnetic Storm, U.T. (11)	Magnitude (12)	Time Interval (13)	(14)
		°					h	
1	Aug. 31·6	20 N.	2300	$(\gamma - \beta\gamma)$	Sept. 2·2	G	+17½	1 and 2
2	Apr. 15·0	21 S.	750	...	None	...	...	3
3	Sept. 25·4	14 N.	1200	$(\gamma$ or $\beta\gamma)$	None	...	...	3
4	Aug. 10·9	8 N.	500	(α)	None	...	...	3
5	Nov. 18·9	19 N.	1711	(γ)	Nov. 17·4	G	+ 7*	3
	,,	,,	,,		Nov. 20·0	G		
					Nov. 21·7	*s*		
6	Nov. 18·9	19 N.	1711	(γ)	Nov. 20·0	G	−16*	3
					Nov. 21·7	*s*		
7	July 14·0	31 S.	829	(α)	July 12·7	G	+30	4
8	July 14·0	31 S.	829	(α)	July 16·5	G	+19½	1 and 2
9	Sept. 9·0	6 S.	494	(α)	Sept. 11·9	G	+26	1 and 2
10	May 13·1	14 S.	108	$(\beta\gamma)$	May 14·2	G	+38	1
	May 13·7	16 S.	681					
11	Sept. 23·8	5 S.	605	$(\beta\gamma - \gamma)$	Sept. 25·5	G	+25	1 and 2
12	Sept. 23·8	5 S.	605	$(\beta\gamma - \gamma)$	Sept. 30·2	*s*	+51	2
13	June 28·8	11 N.	197	(β)	July 1·0	*s*	+38	2
14	Nov. 12·1	24 N.	142	$(\beta$ or $\beta\gamma)$	Nov. 11·8	*s*	+27	1
15	Feb. 9·5	16 S.	2176	β	None	...	...	1
	,,	,,	,,					
16	Feb. 18·3	23 S.	110	β	Feb. 15·6	*s*	+21	1
17	Feb. 18·3	23 S.	110	β	Feb. 15·6	*s*	−27	1
18	Aug. 10·1	16 N.	2389	$\gamma - \beta\gamma$	Aug. 9·2	G	+ 2*	1
	,,	,,	,,					
19	Jan. 24·5	21 N.	3285	$\beta\gamma$	Jan. 26·7	G	+48	1
20	Jan. 24·5	21 N.	3285	$\beta\gamma$	Jan. 26·7	G	+24	1 and 2
21	Feb. 21·4	23 N.	390	$\gamma - \alpha$	Feb. 23·7	G	+37	1 and 2
22	Oct. 13·8	17 N.	527	$\beta\rho$	Oct. 13·8	G	+17†	1 and 2
23	Aug. 12·2	7 S.	349	$\alpha\rho - \beta\rho$	None	...	...	2
24	Apr. 8·0	20 N.	580	$\beta\gamma$	None	...	...	5 and 6
25	Dec. 26·3	19 N.	96	β	None	...	...	5
26	July 15·5	15 S.	148	$\beta\rho$	None	...	...	5
27	Aug. 5·9	24 N.	634	$\beta\gamma$	Aug. 1·9	*s*	+29	5 and 7
28	Oct. 4·4	9 N.	2661	γ	Sept. 30·6	*s*	+ 4	5
29	Jan. 18·4	17 N.	2955	γ	Jan. 22·2	G	+29	5
30	Apr. 14·2	27 N.	1098	$\beta\gamma$	Apr. 13·5	*s*	+ 3	5 and 8
31	Apr. 14·2	27 N.	1098	$\beta\gamma$	Apr. 16·2	G	+21	5
32	Sept. 27·8	12 S.	655	$\beta\gamma$	None	...	...	5
33	Dec. 7·0	9 S.	152	γ	None	...	...	5
34	Apr. 26·4	29 N.	670	β	Apr. 23·2	*s*	+36½	5
35	May 5·3	12 N.	794	$\beta\gamma$	May 5·8	*s*	+34	5
36	Sept. 16·9	11 N.	2000	$(\beta\gamma)$	Sept. 18·2	G	+20½	5 and 9
37	Feb. 28·8	7 N.	2000	γ	Mar. 1·3	G	+19½	5 and 10

† (No. 22, Column 13.) The storm proper does not begin until Oct. 14·7, the listed time Oct. 13·8 referring to a small preliminary disturbance. The mean of the two intervals has therefore been taken.

The headings in Table I are self-explanatory with the help of the following remarks:—

Col. 2. Time (U.T.) when the flare was first observed. Heavy type indicates that the commencement of the flare was actually observed.

Col. 4. The area of the flare, corrected for foreshortening, is expressed in millionths of the Sun's hemisphere. No estimates of areas of bright flares have hitherto been published. Measures of area for the purposes of this table are generally only approximate. Wherever reproductions of spectroheliograms have been published (as in *Ap. J.*, 73, 379, 1931), counts of area by means of a graticule have been made. In recent cases, except nos. 27, 28, 30 and 34, drawings only were available, and these have been measured in the same way. For the earliest flares (nos. 1–7 and 12) a rough value of the area has been given whenever the recorded observations gave some indications, *e.g.* that the *Hα* line was reversed over the umbra or, in other cases, over the penumbra of the associated sunspot, whose area is available from the Greenwich or Kew records. Mr. Evershed kindly lent *Hα* spectroheliograms for the measurement of the area of no. 13. The area of no. 37 is from Mr. Ellison's observations. Several of the estimates given can be improved by observatories holding the requisite spectroheliograms. Only the order of size is aimed at in this column.

Col. 5. The longitude of the flare from the Sun's central meridian is given, longitudes east preceding and longitudes west following the central meridian.

Col. 6. The distance of the flare from the centre of the disk is given as a fraction of the solar radius.

Col. 9. The area is given in millionths of the Sun's hemisphere, and is generally the mean area for the spot's transit of the disk, as given in the *Greenwich Photoheliographic Results*. Areas for nos. 1, 2, 3, 4, 36, 37 are approximate.

Col. 10. The magnetic classification from 1917 onwards comes from the Mt. Wilson publications of sunspot polarities. The type entered in this column before 1917 is to be taken only as a guess at the probable magnetic classification as judged from the recorded appearance of the spot.

Col. 11. The beginning of the magnetic storm ("great" or "small") if within ±2·0 days of the time of the solar flare given in col. 2 (there is one case included with an interval of 51 hours).

Col. 13. The interval between the first observation of the flare and the *beginning* of the magnetic storm is given in hours. In cases when the beginning of more than one magnetic storm has been recorded within the prescribed limits of ±2·0 days, the mean interval, indicated with an asterisk, has been tabulated.

Col. 14. References by which the accounts of the original observations may be traced are as follows:—

(1) *Ap. J.*, 73, 379, 1931.
(2) *M.N.*, 90, 824, 1930.
(3) *J.B.A.A.*, 50, 273, 1940.
(4) *Astronomy and Astrophysics*, 11, 815, 1892.
(5) *Quarterly Bulletin on Solar Activity* (I.A.U.).
(6) *Geomagnetism* (Chapman and Bartels), pp. 341–346.
(7) *L'Astronomie*, 53, 100, 1939.
(8) *M.N.*, 98, 610, 1938.
(9) *Observatory*, 64, 161, 1941.
(10) *Observatory*, 64, 260, 1942.

3. *Discussion of Results*

The results are discussed under two headings: (1) Characteristics of the great solar flares. (2) Their association with geomagnetic disturbances.

Part I. The Solar Flares

These intense flares show certain characteristics under the following headings: (*a*) Frequency, (*b*) Duration, (*c*) Area, (*d*) Light Intensity, (*e*) Spectrum, (*f*) Size, age and type of associated sunspot. Each of the 37 flares was over or closely adjacent to a particular sunspot group; there was no doubt as to which spot group was involved.

(*a*) *Frequency.*—Co-operative observations during the present cycle show that solar flares of intensity 3+ are rare. During nine years of the present cycle, 14 flares of this estimated intensity have been observed in six of the more active years. The true number will be rather larger than this, as some flares will not appear in the 24-hour international record owing to cloud or to certain hours not yet being satisfactorily covered by the I.A.U. observing programme. The correcting factor is unlikely, however, to exceed 2.

Ten of the 37 flares in Table I comprise five pairs of distinct flares, the members of each pair being separated by a day or more, and associated with the same respective sunspot. These pairs are 5 and 6; 7 and 8; 11 and 12; 19 and 20; 30 and 31 (excluding the half-weight units comprising nos. 15 and 18). This suggests a tendency for more than one great flare to occur in the same disturbed area, once it has become active enough to produce an initial great flare. Incidentally, it has been noticed by observers that chromospheric activity is often unrelated to visible changes in sunspots and *vice versa*. The size of a sunspot is not always a criterion of associated chromospheric activity, some large sunspots being relatively inactive in this respect.

(*b*) *Duration.*—The duration of flares in Table I ranges in the best observed cases from just under 1 hour (excluding the special case of 1859 September 1) to 3 hours and over. This duration is considerably longer than the mean of about $\frac{3}{4}$ hour for flares of intensity 3.

(*c*) *Area.*—The areas at maximum development are comparable with those of the larger sunspots and sometimes exceed the greatest ones. Nos. 19 and 20 were of notable extent. Unusually rapid changes of form and area were noted by observers of nos. 3, 11 and 21. The emission area is often an amorphous patch, but sometimes the structure is in streaks as in nos. 3, 21, 25 and 37.

(*d*) *Light Intensity.*—Quantitative measures are nearly entirely absent, the observers describing specific flares as, for example: "Both C, F and the line near D *were magnificently bright on the Sun itself*" (Norman Lockyer, no. 2). Hale describes flare no. 20 as "extremely brilliant . . . the most remarkable solar phenomenon I have ever seen." In at least three instances (nos. 3, 8 and 11) the brilliant form of the flare could be seen in *Hα* on the disk through the widened slit of a spectroscope. The flare of 1938 December 7 (no. 33) is stated by Mount Wilson to have been exceptionally brilliant. Measures of peak intensity were made at Greenwich with a wedge photometer on flares 25 and 36. In both cases the peak intensity of the *Hα* line in emission just exceeded that of the continuous spectrum 15 A. from its centre. From other photometer measures made at Greenwich on flares of intensity 3, it is found that the peak intensity equals or exceeds (sometimes by 50 or 100 per cent.) that of the solar spectrum beyond the wings of the *Hα* line. Thus, flares of intensity 3+ may not be markedly distinctive in their light intensity per unit area as compared with flares of intensity 3, but the integrated intensity of the former over their extensive area must greatly exceed that of the latter. Intensity measures on all brilliant flares are therefore of primary importance in conjunction with area measurements. The method of using the effective line-width of the *Hα* reversal as shown by Giovanelli, Waldmeier and by Ellison will give useful data to be converted into a light intensity scale. With improved technique, it is possible that intensities of solar flares might be assessed from the radial velocities of rapidly moving absorption markings (prominences in projection) often found associated with flares.*

There is need also of a geophysical measure of the intensities of solar flares based on the synchronous radio fade-out and magnetic disturbance (shown by a "crotchet" on the magnetic traces). Since the Sun's zenith distance at the place of observation is a governing factor in the local occurrence of the dual geophysical phenomena, ionospheric and magnetic records from various stations must be available for a consistent assessment of the intensity of solar flares. In each of the cases in Table I the Greenwich magnetic traces have been examined. Of the 37 flares, 12 occurred at times when the Sun was either below the horizon at Greenwich or not far from it, so that in these cases "crotchet" perturbations would not be expected. Of the 25 cases for which the solar altitude did not preclude the recording of crotchets, there were only 12 cases of possible crotchets, as follows:—

* *M.N.*, 102, 1 and 11, 1942.

Ref. No. of Flare	Date	"Crotchet" begins U.T.	Range D	Range H
		h	′	γ
1	1859 Sept. 1	11·3	+16	−110
6	1882 Nov. 21	10·7	Nil	− 22
7	1892 July 11	11·7	+12	− 30
8	1892 July 15	17·2	+ 2	+ 8
10	1909 May 12	13·3	+ 4	Nil
11	1909 Sept. 24	11·0	Lost trace	− 40
22	1926 Oct. 13	13·8	+ 5	− 13
23	1930 Aug. 12	11·0	− 2	− 6
24	1936 Apr. 8	16·7	− 2	Nil
28	1937 Sept. 30	10·3	− 6	− 8
36	1941 Sept. 17	8·4	− 6	− 25
37	1942 Feb. 28	12·0	+ 4	− 70

Notes

It is doubtful whether nos. 8, 10 and 23 are true "crotchets." For no. 24, the recorded range in H at Huancayo (latitude 12° S., longitude 5 hours W.) was $+108\gamma$ in 5 minutes, followed by a decrease of 139γ in the next 37 minutes. In no. 37, one of the best examples, the fade-out and the crotchet began within 30 seconds of one another. The time of origin of the solar flare was not observed, but it was seen as soon as the clouds broke.

In addition to the above, there was a typical "crotchet", recorded at Kodaikanal (latitude 10° N., longitude 5 hours E.), synchronous with solar flare no. 12; the range in H was $+154\gamma$.*

As regards synchronous fade-outs, since 1936 when collective ionospheric data became available, each of the solar flares nos. 24–37 was associated with a fade-out recorded on wave-lengths from about 13 to 50 metres. The mean time-difference, *fade-out begins—solar flare first seen*, was −5 min., but in the six cases when the beginning of the flare could be timed, the corresponding mean time-difference was +10 min. Though the occurrence of a synchronous fade-out indicates † that the solar flare was probably of intensity 3, the present data do not discriminate between flares of intensity 3+ and 3, though the duration of the fade-out may afford a partial criterion.

(*e*) *Spectrum.*—The spectra of flares have been studied ‡ by Richardson and Minkowski and by Allen. Richardson concludes that "there appears to be no essential difference in the spectral characteristics of the eruptions; that is, an eruption of intensity =3 differs from one of intensity =1 only in brightness." But in Richardson's table of lines affected, there are some notable omissions (including D_1D_2 and *b* group) which appear in Allen's table. Richardson also states that the helium line D_3, which frequently shows as a faint absorption line on the Sun's disk over spot groups, could not be detected as an emission line on any of the photographs taken for his investigation. Allen, however, gives this line in his table of emission lines from visual observations of various flares (dates unspecified).

The following lines have been seen in emission, sometimes brilliantly, by observers of flares recorded in Table I, in addition to the brilliant reversals of $H\alpha$ and $H\beta$:—

1870 *September* 28 (Young).—D_3 reversed over sunspot umbra.

1882 *November* 18 (Maunder).—$D_1D_2 : D_3$ reversed over sunspot umbra. D_1 and D_2 were greatly broadened, each line appearing as a very broad and ill-defined dark band about 6 A. in width, with a sharp, narrow emission line in the centre.§ The great broadening of D_1 and D_2 was also observed by Maunder in the flares of November 20 and 21, although the thin central reversal was not seen, probably owing to bad observing conditions. D_3 was seen in emission over the sunspot penumbra on November 21 and was suspected to be in reversal over the umbra on November 20, at which places $H\alpha$ was seen in emission.

* *M.N.*, 70, 24, 1909.

† *M.N.*, 97, 605, 1937.

‡ *Ap. J.*, 89, 347, 1939; *M.N.*, 100, 635, 1940.

§ *M.N.*, 43, 78, 1883.

1892 *July* 11 (Townsend).—D_1D_2 : D_3 and the *b* group were all brilliantly reversed over the spot umbra. Another line, given as 6676·9 in Rowland's map, was also seen in emission. This line may be the *He* line 6678·10 A. given as one of the emission lines in Allen's table. There is a strong *Fe* line at 6678·01.

1909 *September* 24 (Fowler).—b_3 was seen in emission over the sunspot umbra.

1909 *September* 28 (Kodaikanal).—D_1D_2 : D_3 and the *b* group seen in reversal over spot umbra. Evershed points to the behaviour of other lines as evidence of an abnormal magnetic field in the sunspot at the time of the flare.*

1926 *January* 25 (Hale).—D_1D_2 : D_3 brightly reversed over giant sunspot. D_3 was seen as an absorption marking beyond the spot itself.

1926 *February* 22 (Kodaikanal).—D_1D_2 and *b* lines reversed near sunspot umbra. D_3 in absorption north of sunspot.

1926 *October* 13 (Meudon).—D_3 reversed in region of flare.

Richardson and Minkowski obtained spectra of flare no. 33 on 1938 December 7. A bright streak appears in the visual region of the spectrum of the flare but *not* at the position of the line emission.† It is suggested here that this interesting feature, if reobserved in future flares, might give a clue to the brilliant patches of 1859 September 1, seen in integrated light.

It is obvious from these brief notes that the study of the spectra of the brightest flares should be continued in order to clear up existing discrepancies and to see whether flares of great intensity have special characteristics in their spectra.

(*f*) *Size, Age and Type of Associated Sunspot.*—Though the data in Table I show that many of the great flares are associated with great sunspots, there are also some smaller spots with mean area less than 500 millionths. In *The Observatory*, **62**, 325, 1939, Fig. 5, there is a comparison of the distribution of the sizes of sunspots observed with (1) Flares of intensity 3+ and 3, 1935–1938. (2) Great magnetic storms, 1875–1938. The distribution in the two sets of data is similar.

The frequency curve for the ages of sunspots at the time when flares of intensity 3+ and 3 occur over them shows a marked peak at the phase of maximum growth of sunspots (*loc. cit.*, p. 325, fig. 6). Although less intense flares may often be seen during the initial growth of a spot group, the more intense flares favour this phase least of all.‡

Column 10 of Table I shows that the majority of the associated spot groups have a complex distribution of magnetic polarities as indicated by γ or $\beta\gamma$. This preference may, however, merely reflect the tendency for great spots to be of γ type.

No. 21 is, however, an interesting case of a medium-sized spot having a γ classification for part of its transit, and though perhaps only an accidental occurrence, it may be noted that the type changed from γ (complex) to α (unipolar) during the 24-hour interval when the flare occurred.

Part II. Association with Magnetic Storms

An examination of Table I, col. 11, shows that out of 37 solar flares, magnetic storms began within ±2·0 days in no fewer than 27 cases. For the central part of the disk (0°–45° longitude from C.M.) the degree of association was even higher, viz. over 80 per cent. Two-thirds of the storms associated with flares in this central zone are, moreover, "great" storms. All the great storms occurring in Table I are associated with flares within 0·71 of a solar radius, or 45° from the centre of the disk.

Great storms as well as intense solar flares are infrequent phenomena. On the

* *Kodaikanal Bulletin*, **22**, 265, 1910, and (Michie Smith) *M.N.*, **70**, 23, 1909.

† *Ap. J.*, **89**, 353, 1939.

‡ Giovanelli in *Ap. J.*, **89**, 555, 1939, gives statistics of the incidence of flares with respect to the size, age, and polarity type of sunspots, but flares of intensity 3 have not been analysed separately.

average, during the years represented in Table I, there were 3·2 great storms per year. There are listed 28 intense flares in the central zone of the Sun's disk. It follows that the total number of chance coincidences of a flare day occurring within ±2·0 days of a commencement day of a great magnetic storm is $28 \times 3{\cdot}2 \times 4 \div 365$ or approximately 1. The number of coincidences found is 17 (flares nos. 19 and 20 are, however, both listed with the same magnetic storm). For small storms, the corresponding number of chance coincidences is $4\frac{1}{2}$, the observed number being 6, not counting the small storm of 1882 November 21, which occurs near a great storm.

The significance of this statistical result is enhanced by the fact that in every case except one the great magnetic storm came after the flare. The mean statistical interval, *magnetic storm begins—solar flare begins*, is $21^{h}{\cdot}5 \pm 2^{h}{\cdot}1$, including all storms in Table I.

These results are strong evidence in favour of a close relation between intense solar flares and great magnetic storms, and the evidence is strengthened by the results given by the "superposed epoch" method of analysis of the data. Taking the day of each

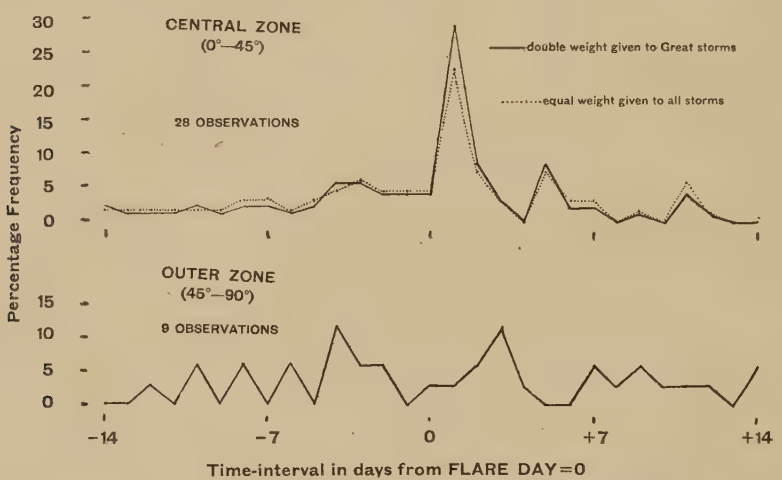

FIG. 1.—*Magnetic storm frequency around day* (=0) *of intense solar flares.*

flare in Table I in turn as day 0, each magnetic storm that *began* on any of the days −14 to +14 (thus comprising a solar synodic rotation) was taken as counting 1 for the appropriate day. This horizontal tabulation was done for each of the solar flares, those occurring within 45° of the central meridian being tabulated separately from those in the outer zone of the Sun's disk. The vertical columns were then summed and percentages taken. The results are graphed in Fig. 1.

It will be seen that:

(*a*) For the central zone there is a single peak at about one day after the mean solar flare. This peak is heightened if double weight is given to the great storms, and rises to nearly 45 per cent. for the percentage frequency of great storms if this is plotted separately.

(*b*) For the outer zone no definite single peak is shown.

(*c*) From the analysis of the central-zone flares the following points were also noted: (1) The three great magnetic storms of 1926 February 23, October 13 and 1941 September 18, were the only storms recorded at Greenwich within ±10 days of the respective associated solar flares. (2) For a pair of flares, viz. nos. 7 and 8, there was a corresponding pair of great magnetic storms, and no others within ±10 days. Another pair of flares, nos. 30 and 31, was answered by a pair of isolated storms, but not both "great." After a third pair of intense flares, nos. 19 and 20, there was, however, only one great storm. (3) The small magnetic storms of 1916 July 1 and 1917

February 15 were the only ones within ±14 days of the respective solar flares, nos. 13, 16 and 17.

Great Magnetic Storms.—Bearing in mind the necessarily broken nature of the solar record, the data presented in Table I and fig. 1 indicate that, for great magnetic storms (at least), there is a high probability of an intense solar flare about one day before the beginning of a storm. Although in Table I there are some small storms * associated with intense flares, there is a special difficulty in ascribing the occurrence of lesser magnetic storms as a class to antecedent flares. Near solar minimum, the observed frequency of flares of intensity 3+ apparently falls to zero, whilst those of intensity 3 or even 2 are very infrequent. Now, throughout sunspot minimum, small magnetic storms continue to occur, often in sequences of 27 days. It would seem, therefore, that the corpuscular streams responsible for great storms and for small storms differ in their circumstances of emission from the Sun so far as visible disk phenomena are concerned.

Time-Interval.—The statistical mean time-interval given by all the data in Table I is $21^h.5 \pm 2^h.1$. Confining our attention to the great storms, if ambiguous cases † be omitted, the derived time interval is $25^h.7 \pm 1^h.5$. If it be assumed that the ejection of a corpuscular stream occurs at or near the beginning of the solar flare (whose maximum usually occurs within 10 minutes of its sudden beginning), then this interval represents the effective time of travel (T_e) of the stream from Sun to Earth. This value of $25\frac{1}{2}$ hours accords with that derived from sunspot statistics without knowledge of solar flares, *e.g.* from the central meridian passage time of great spots associated with the commencement times of 19 great magnetic storms (1875–1903), Maunder ‡ derived a mean time-lag of 26 hours. Observationally, there appears to be a tendency for the most intense magnetic storms to give a shorter value of T_e than the average. From the five greatest magnetic storms included in the present discussion, for which there are the requisite solar-flare data, the value for T_e is $20^h.4 \pm 0^h.9$. These greatest storms are related to flares nos. 1, 11, 31 and 36. Included in the mean is a fifth value of $T_e = 18^h$ derived from the great storm of 1941 March 1. The associated flare was not actually observed, but it is almost certainly indicated by a radio fade-out and a synchronous crotchet on the Abinger magnetic traces.§

Distribution on Sun's Disk of Flares prior to Great Storms.—The positions on the Sun's disk of the solar flares in Table I, associated with great and small magnetic storms, are plotted in Fig. 2A. Small storms so associated are plotted with open circles. The small circles represent half-weight observations. In Fig. 2B are plotted the positions of inferred flares preceding other great magnetic storms recorded at Greenwich since the solar maximum of 1870. These data are derived as follows: The statistical relationship between the occurrence of magnetic storms and the central meridian passage of large sunspots is best shown by the greatest storms.‖ In most of these cases a large sunspot is somewhere in the central zone of the disk when the storm begins. The present analysis has shown the probability that a great storm is preceded by an intense flare about 20 hours earlier. Thus, the position of a great, or otherwise distinctive sunspot 20 hours before the storm begins will give the most probable position of the solar flare. In this way the crosses in Fig. 2B have been derived for all the "very great" storms not already in Table I. In one case (1903 October 31) the sunspot of greatest mean area was near the east limb, but South Kensington spectroscopic observations ¶ indicate clearly

* Two of these small storms with a mean range of 224 γ (1939 April 23) and 205 γ (1939 May 5) missed the minimum range in H for a great storm by only 10 γ and 15 γ respectively. A third storm (1909 September 28) had a mean range of 209 γ.

† Nos. 5 and 6 (multiple storms); no. 18 (dual flares); nos. 19 and 20 (1 storm); no. 22 (beginning of storm indecisive).

‡ *M.N.*, 64, 206, 1904.

§ *The Observatory*, 64, 82, 1941.

‖ *M.N.*, 88, 559, 1928.

¶ *Nature*, 69, 6, 1903; *M.N.*, 64, 38, 1903.

the active nature of the rather smaller group within the central zone. A brilliant reversal of *Hα* observed on October 30 might have been included in Table I had fuller data been available. For a second storm, viz. 1870 May 20, two half-weight points (small crosses) have been plotted, representing two spot groups of about equal size.

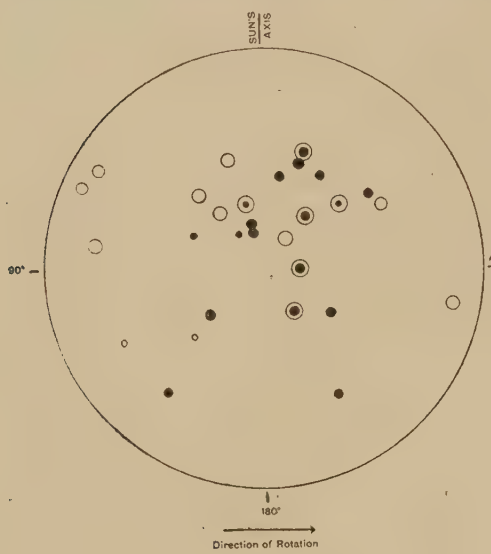

FIG. 2A.—*Position on solar disk of observed flares preceding magnetic storms.*

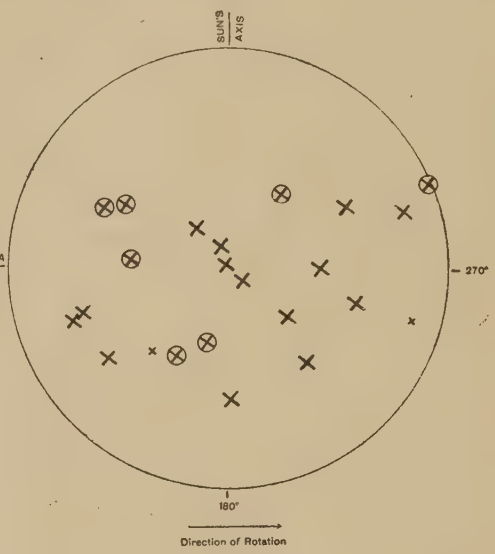

FIG. 2B.—*Position on disk of "deduced" flares preceding "very great" magnetic storms.*

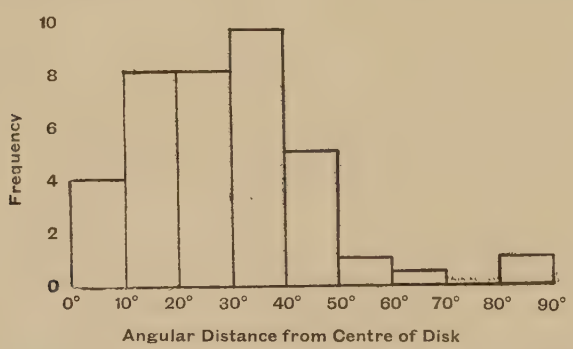

FIG. 3.—*Distribution on Sun's disk of flares associated with great magnetic storms.*

From the combined data in Figs. 2A and B, which represent the positions of the flares as seen on the disk (projected areas), the frequency distribution (corrected) of angular distance of the points from the disk centre is obtained in Fig. 3 by tabulating the respective values of $\sin^{-1}(r/R)$.

The following points are suggested by the data in Figs. 2 and 3:—

(1) There is a central zone of the Sun's disk from which (both east and west of the C.M.) corpuscular streams can reach the Earth to produce magnetic storms. The most frequent angular distance from the disk centre is 20°–40°, and there is a sudden drop between 40° outwards to the edge of the disk. The partial drop from about 10° to the centre—the most favourable position for a corpuscular stream to impinge on the Earth, neglecting the aberrational effect of T_e—may be due to the relative infrequency

of sunspots within a few degrees of the equator. Likewise, the apparent tendency for a lateral distribution, roughly east to west, of the points in Fig. 2 may be due to the relative infrequency of spots in latitudes higher than 25°.

The limits thus found for the effective central zone of the disk associated with the occurrence of great magnetic storms agrees with those obtained from data (1874–1927) of mean areas of sunspots given in *M.N.*, **89**, 88, 1928, Table III. The effective lunes shown in that table by the last three classes of storms of increasing mean intensity are 26° E.–53° W. of the Sun's central meridian. Allowing $T_e = 1$ day or 13° of solar longitude, the limits become 39° E.–40° W.

(2) The intensity of a magnetic storm following an intense solar flare situated within this area of about 45° radius does not seem to depend to any appreciable extent upon its position within the area. This is borne out by the positions of flares plotted for the outstanding storms of the last 85 years * which are indicated by the ringed dots and crosses. On the other hand, some dependence upon position within the central zone may be indicated by the fact that the most extensive flares as yet recorded (nos. 19 and 20 occurring at 26° and 31° respectively from the disk centre) were followed by only one great storm, not of unusual severity.

(3) The general distribution of points within the area of about 45° radius, especially the absence of a marked excess of points east (preceding) over points west (following) with respect to the central meridian, suggests that corpuscular streams producing great magnetic storms encounter the Earth largely "head-on," *i.e.* the part of the Earth's orbit first reached by the outward moving stream includes the Earth itself. The case is apparently different for the smaller storms (those with mean range < 180 γ at Greenwich, below which limit the recurrence tendency definitely appears). In order to explain their tendency to recur at intervals of a solar synodic rotation, it is assumed that the corpuscular stream, ejected more or less continuously for a considerable time and partaking of the Sun's rotation, overtakes the Earth in its orbit (see *Geomagnetism*, p. 412). The absence of an appreciable tendency for great storms to recur in about 27 days †, is an important distinction in connection with the results found in this paper. In at least one case when a great storm was followed by another some 27 days later (1926 January 26 and February 23), a second intense flare was actually observed before the second storm (no. 21 in Table I). From the analysis of sunspot statistics, Greaves and Newton ‡ suggested that for the more intense magnetic storms, "the solar disturbance from which the stream is being ejected is, in general, short-lived and does not survive a solar rotation in an appreciable number of cases." Other explanations have been suggested by Chapman and by Bartels.§

A hypothetical division of magnetic storms into two types, (*a*) nascent-stream type, (*b*) mature-stream type, has been suggested by Bartels.‖ The magnetic storms connected with the solar flares plotted in Fig. 2 would be identified generally with type (*a*), in which the freshly formed corpuscular stream, as Bartels suggests, in sweeping across the Earth's orbit hits the Earth directly. In these cases the observed duration of the magnetic storm would be related to the actual duration of emission of the corpuscles from the Sun and any range of velocities of the corpuscles within the same stream, although the effect of the Sun's rotation imparted to the stream would be a factor. The time interval T_e for these storms would approach the true time of travel of the head of the stream from Sun to Earth.

It may here be noted that the time of travel derived from Milne's theoretical work on the ejection of high speed atoms from the Sun under radiation pressure is 1·1 days.¶

* Beginning on—1859 Sept. 1; 1872 Feb. 4; 1882 Nov. 17 and 20; 1903 Oct. 31; 1909 Sept. 25; 1921 May 13; 1938 Jan. 25; 1938 Apr. 16; 1940 Mar. 24; 1941 Mar. 1; 1941 Sept. 18.

† *M.N.*, **89**, 641, 1929; *Observatory*, **63**, 47, 1940. ‡ *M.N.*, **89**, 643, 1929.

§ *Observatory*, **52**, 168, 1929; *Terrestrial Magnetism*, **45**, 342, 1940.

‖ *Terrestrial Magnetism*, **45**, 339, 1940. ¶ *M.N.*, **89**, 458, 1929.

With reference to the suggestion of two types of storms, it should be remembered that Chapman has pointed out that the general character of the field and its changes are apparently the same over a fourfold range of intensity, though the rate of progression of the field through its successive phases depends to some extent on the intensity of the storm.*

(4) The angular extent of the area of the disk in which those flares associated with magnetic storms occur, indicates that the semi-angle of the equivalent cone of a solar stream on encountering the Earth can be as great as 45°. An alternative explanation would be that the streams are usually much narrower, but are ejected within a wide angular range from the normal to the chromosphere. The high percentage of solar flares in Table I followed by great magnetic storms does not, however, favour this view. The present evidence suggests, in fact, that when a great sunspot within the

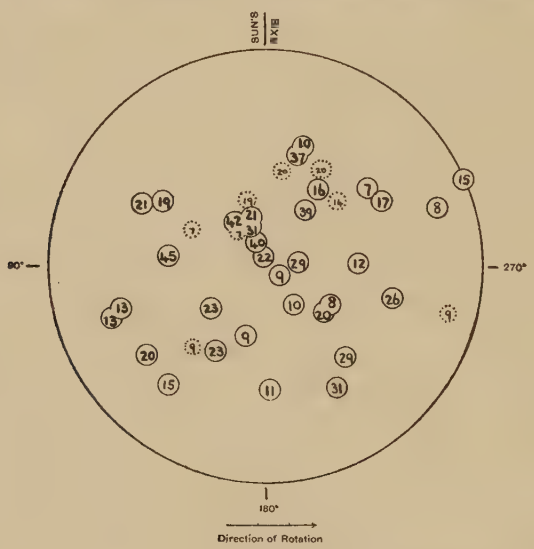

FIG. 4.—*Positions on disk of flares (combined data) with storm duration in hours of great storms.*

central zone of the disk is not accompanied by a great magnetic storm, the reason is to be attributed to the absence of a corpuscular stream at that time rather than to the Earth's just missing a narrow but continuously ejected stream, though this may well happen occasionally.

Chapman † derived an angular width of the order of 25° (semi-angle of equivalent cone $12\frac{1}{2}°$), but this estimate is based on the average duration of a magnetic storm, assuming that the stream overtakes the Earth on the *post meridiem* side, as would be the case with the mature-stream type storms.

There is one outstanding position in Fig. 2B, at 0·99 and 293°, related to the very great storm of 1938 January 25. Solar flares, including two of intensity 3, were actually observed on the previous day near the position plotted where the largest sunspot on the disk was only about 5° from the Sun's limb. Though a flare of intensity 3+ might have escaped detection within the central zone, there is no evidence for this assumption, and the available data given in the Zürich *Solar Bulletin* point to the active region near the limb as the source of the corpuscular stream. This implies that on rare occasions the corpuscular stream may be either abnormally wide or be ejected at a large angle from the normal and still reach the Earth.

Finally, it is of interest to see whether the duration of a great magnetic storm is

* *Geomagnetism*, p. 280.

† *Geomagnetism*, p. 414.

related to the position on the disk of the antecedent flare. For this purpose the storm duration has been taken as the interval between the abrupt commencement and the ending of the more violent deflections on the magnetic traces. The flare positions and these storm durations are shown in Fig. 4. Dotted circles represent half-weight observations.

(*a*) The mean storm duration for points east is 22 hours and for points west of the central meridian 18 hours. The reality of this difference is doubtful in view of the probable error of about $\pm 2^h$ for the mean durations.

(*b*) The disk has been divided by circles concentric with the limb into two zones, inner (up to 27°) and outer, each containing about the same number of points. The respective mean durations are 22 hours and 18 hours. The difference is qualitatively in the expected direction but is uncertain because of the probable errors.

Acknowledgments.—I gratefully acknowledge the Astronomer Royal's permission to assemble and discuss the material comprising this paper. Dr. A. Hunter kindly discussed with me the question of solar flare spectra. Mr. H. Barton and Mr. P. Laurie made the area measurements given for flares in Table I, and Miss C. Chapman, also of the Observatory staff, helped in preparing the data for publication. Finally, it is a pleasure to acknowledge Professor S. Chapman's helpful remarks included in the revision of the MS.

Royal Observatory,
Greenwich:
1943 *August* 6.

INTENSITIES OF HYDROGEN *Hα* AND HELIUM D_3 IN PROMINENCES

H. A. Brück and W. Moss

(Received 1943 October 6)

Summary

The observational procedure is described by which equivalent widths of *Hα* and D_3 and their local variations in prominences are determined. First results for nine prominences are in good agreement with earlier observations of Minnaert and Slob. Within one and the same prominence the intensity ratio $H\alpha/D_3$ is found to decrease with increasing intensity of D_3, indicating the effect of self-absorption on *Hα*. In the brightest prominence here investigated *Hα* is about eight times fainter than it would be without that effect being present. Intensities of *Hα* when plotted against intensities of D_3 are consistent with the theoretical curve of growth which corresponds to thermal motion without turbulence.

---

1. *Introduction.*—Investigations of line intensities in prominences have been made by several observers, and the lines hydrogen *Hα* and helium D_3 have been studied in particular by Perepelkin * and by Minnaert and Slob.† Perepelkin's intensities are based on visual estimates, and Minnaert and Slob have been the first to determine, photometrically, values of equivalent width for both lines in three prominences at different levels above the solar limb. These observers found the intensity ratio $H\alpha/D_3$ to decrease with increasing intensity of D_3, but contrary to Perepelkin they did not detect any definite correlation between that ratio and the level in the prominence. More recently Minnaert and Slob's results, together with their unpublished measurements on three more prominences, have been discussed by Unsöld.‡

In the summer of 1941 comparisons of *Hα* and D_3 in prominences were made by Thackeray with the spectrohelioscope of the Solar Physics Observatory, Cambridge. Thackeray noted differences in structure as Lyot § had seen them, and observed frequently low-lying chromospheric spikes with exceptionally strong helium lines. To obtain some photographic confirmation of his visual observations he also made simultaneous photographs of *Hα* and D_3 with the Rowland concave grating.

2. *Observations.*—In view of the theoretical interest of such observations and of the scarcity of the material so far available, a programme of observations was started by the present writers in the spring of 1942; in the course of this a number of equivalent widths of *Hα* and D_3 have been and are being secured for different types of prominences and in various regions of one and the same prominence. This work was started with the Rowland concave grating, but because of difficulties connected with the identification of points within one prominence and also with the photometric procedure, the spectroheliograph was soon chosen as being a more suitable instrument for the purpose.

The set-up of the spectroheliograph was rearranged so that the spectra in both cameras are now produced by the same Rowland plane grating, which, by means of suitably placed mirrors, throws the spectral region near *Hα* into the first and the region near D_3 into the second camera. Spectra from both sides of the central image from the

* *Z. f. Physik*, 49, 295, 1928.
† *Pr. R. Ac. Sc. Amst.*, 33, 65, 1930.
‡ *Physik der Sternatmosphären*, p. 409, 1938.
§ *C.R.*, 202, 392, 1936.

grating have to be used in this arrangement; originally *Hα* was photographed in the second and D_3 in the first order with dispersions of about 5 A./mm. and 10 A./mm. respectively. This arrangement has been altered recently, and the second order is now used for both spectra. The normal secondary slits of the spectroheliograph are in position, but are kept about a millimetre wide, allowing a spectral range of about 6 A. to fall on the photographic plates.

The observational procedure is as follows. When visual observations in *Hα*, through a finder attached to the spectroheliograph, have shown the presence of one or more prominences, the spectroheliograph is brought into position, and, by means of a micrometer screw, moved across the whole extent of the prominence while its appearance is watched visually. The movement is in equal steps of a fraction of a millimetre, and at each step simultaneous photographs of *Hα* and D_3 are taken with the two cameras. Plates carry therefore primarily a set of up to 20 spectra ("cuts") of one prominence or several shorter sets when more than one prominence is visible and when all prominences are to be taken on the same plate. The photographs include a narrow region of the spectrum of the solar limb, whereas the light of the rest of the Sun is eliminated by a metal disk placed in front of the primary slit.

In addition to the set of "cuts", spectra of the centre of the Sun are taken on the same plates and with the same exposure time. These serve to transform equivalent widths of *Hα* and D_3 into units of the intensity of the continuous spectrum near the lines at the solar centre; on account of the effects of seeing, this is preferable as reference spectrum to the spectrum of the solar limb. To reduce the intensity of the spectrum of the solar centre, the 12″ Cooke object-glass is stopped down to a diameter of 4″, and a Zeiss step-wedge, whose transmission has been carefully determined photo-electrically, is placed in front of the primary slit.

Additional exposures through the same step-wedge provide the means for standardisation and determination of characteristic curves.

To reduce the considerable difference in intensity between *Hα* and D_3 which would make accurate photographic photometry impossible, Wratten colour filters * have been introduced into the two cameras; their relative transmissions, together with the relative sensitivities of the photographic plates employed, secure comparable photographic densities for *Hα* and D_3. As all intensities are referred to that of the spectrum of the solar centre, and since this is equally affected by these filters, no absolute determination of the transmissions of the filters is required.

Ilford Astra VIII plates are used for the exposures on *Hα*, and Ilford Thin Film or Process (in one case Rapid) Panchromatic plates for those on D_3. Each pair of plates is developed together for 6 minutes in M-Q developer.

3. *Photometric Procedure and Reduction.*—Photographic densities on the plates are measured in the normal way with the Cambridge recording microphotometer. The different sets of cuts are run through in the direction of dispersion, the distance of the photometer slit from the spectrum of the solar limb being measured in each cut with a micrometer screw. All tracings are made with a slit width of 0·01 mm. The slit length is varied between a few tenths and half a millimetre according to the dimensions of the prominence on the plate.

Both emission lines *Hα* and D_3 are seen as superimposed on spectra of the sky, and in the determination of intensities allowance must be made for the presence of this background spectrum, whose intensity decreases with increasing distance from the solar limb and which also varies with atmospheric conditions.

Intensities of *Hα* and D_3 have been expressed in terms of equivalent width; the unit of equivalent width is taken to be equal to the energy contained within a spectral range

* The writers want to express their sincerest thanks to Mr. D. R. Barber and to the Research Laboratories of Kodak, Ltd., for their great kindness in supplying them with special photographic material for experimental exposures.

of 1 A. of the continuous spectrum of the solar centre near the lines. The procedure adopted has been first to compare the intensities of emission with the intensity of the underlying spectrum of the sky, and then to compare this with the intensity of the spectrum of the solar centre. The method is simple for the D_3 line where the sky spectrum is purely continuous, and the accuracy of results is only impaired in the case of weak prominences superimposed on relatively strong sky spectra. In the case of $H\alpha$, allowance has to be made for the presence of the $H\alpha$ absorption line within the sky spectrum. Additional tracings have been made of this line as it is produced by the spectroheliograph on the different plates, and the intensity distribution within the line has been derived for all the plates which are considered in this paper.

For the purpose of reduction the intensity distributions within both the $H\alpha$ and D_3 emission and also within the core of the $H\alpha$ absorption line have been represented by triangular contours.

4. *Results.*—So far more than a hundred pairs of plates have been secured. Ten particularly good pairs obtained in recent months have been selected for this first paper, which is to be followed by a more comprehensive study of the available material. With the exception of the first three plates (see Table I) the selected material is representative of prominences with one or two well-defined streamers running outward from the solar limb; their course has been followed photometrically. The first two plates of Table I refer to one prominence of the active type which has been studied in two different regions (corresponding to (*a*) and (*b*)) and at different levels, and which has been photographed again after an interval of one hour and twenty minutes (Plate 2). Plate 3 also refers to a large prominence of the active type which has been studied with two sets of cuts. Normal spectroheliograms in $H\alpha$ of the solar limb help to show the structure of five of the nine prominences in the table. Such pictures have been generally obtained when there was time available.

The second column in Table I shows the heights above the solar limb of those regions in the prominences which have been investigated. These heights correspond to the measured positions of the photometer slit relative to the base of the prominences. The extension of the different cuts in height depends both on the slit length and on the latitude of the prominence. The actual range of each cut in height is in all cases smaller than half the distance between two consecutive cuts. Bad seeing makes the determination of heights rather difficult, and there may be considerable systematic errors in the given values, particularly between different plates. On account of the unknown effect of foreshortening, heights in different prominences cannot in any case be compared directly.

The next three columns of the table give the equivalent widths of $H\alpha$ and D_3 in units of 10^{-2} A., under headings $I(H\alpha)$ and $I(D_3)$, and their intensity ratio, $H\alpha/D_3$. The meaning of the last column will be explained later.

The average values of equivalent widths for $H\alpha$ and D_3 in Table I agree well with Minnaert and Slob's observations. Prominences studied in this paper cover a rather wider range of intensities. As had already been observed by Minnaert and Slob, intensity ratios $H\alpha/D_3$ are seen to vary both with height and with intensity of D_3, decreasing rapidly with increasing intensity of helium. Particularly high values of $H\alpha/D_3$ are found in the table for those prominences which are about ten times fainter than the faintest ones observed by Minnaert and Slob.

Fig. 1 indicates, for some of the prominences, the decrease in the intensity ratio of $H\alpha/D_3$ with increasing intensity of D_3; the corresponding curves for the three prominences studied by Minnaert and Slob are given for comparison.

The data show that the values of $\log(H\alpha/D_3)$ for each prominence can be well represented by linear functions of either $\log I(D_3)$ or of height. It has been shown to be probable already by Minnaert and Slob that the intensity ratio $H\alpha/D_3$ is primarily dependent on intensity, and that the observed variations of $H\alpha/D_3$ with height can be explained largely, if not wholly, by the dependence of the intensity on height.

TABLE I

Intensities of Hα and D_3 in Various Regions of Nine Prominences
(expressed in units of 10^{-2} A.)

Plate	Height in 10^3 km.	$I(H\alpha)$	$I(D_3)$	$H\alpha/D_3$	k
1 (*a*)	18	14·6	0·85	17	
	24	15·7	1·46	10	
	29	12·2	0·64	19	0·60
	36	9·7	0·34	28	
	42	4·5	0·10	45	
(*b*)	25	33·0	1·62	20	
	33	29·5	0·78	38	0·00
	39	19·0	0·30	63	
	46	8·6	0·08	101	
2	39	5·02	0·46	11	
	46	3·97	0·30	13	0·92
	52	3·26	0·18	18	
3 (*a*)	5	7·30	0·125	58	
	16	2·22	0·023	97	0·15
	27	3·94	0·039	101	
	38	2·80	0·025	112	
(*b*)	4	7·38	0·224	33	
	9	5·98	0·220	27	
	18	5·13	0·095	54	
	28	5·91	0·142	42	
	39	4·75	0·113	42	(0·30)
	51	4·77	0·071	67	
	61	4·51	0·040	113	
	72	3·20	0·028	115	
4	13	9·16	0·23	40	
	21	9·40	0·24	39	
	28	10·60	0·26	41	
	33	8·85	0·22	40	0·40
	45	7·55	0·17	44	
	68	6·08	0·13	47	
	87	5·80	0·15	39	
5	16	0·86	0·027	32	
	26	1·53	0·081	19	
	31	2·62	0·135	19	0·82
	35	1·46	0·085	17	
	38	0·46	0·013	35	
6	14	9·85	0·170	58	
	22	6·25	0·076	82	0·10
	30	2·92	0·032	91	
	41	2·66	0·022	121	
7	48	3·34	0·41	8	
	50	5·45	1·96	3	(1·32)
	55	4·91	0·90	5	
	57	4·70	0·75	6	
8	6	14·4	0·47	31	
	10	9·8	0·18	54	0·32
	14	7·6	0·14	54	
	21	4·8	0·10	48	
9	4	4·45	0·26	17	
	10	2·80	0·15	19	0·77
	16	2·30	0·11	21	
10	16	7·29	0·157	46	0·32
	23	4·57	0·065	70	

For the longer sets of cuts in Table I (say for the set 3 (*b*)) partial correlation coefficients can be determined between the values of log $(H\alpha/D_3)$, log $I(D_3)$ and height. Significant values are found only for the coefficient of partial correlation between sets of log $(H\alpha/D_3)$ and log $I(D_3)$.

The observed decrease in the relative intensity of $H\alpha$ with increasing intensity of D_3 can be quantitatively explained by the effect of self-absorption on $H\alpha$. It is assumed that within one prominence relative numbers of hydrogen atoms responsible for emission of $H\alpha$ can be represented by a Boltzmann distribution at the temperature of

the solar boundary; the total energy emitted in $H\alpha$, expressed in units of the energy in the continuous solar spectrum near the line for the boundary temperature, must then be equal to the energy absorbed within the same line. The first is identical with our definition of equivalent widths and with the values of $I(H\alpha)$ in Table I, apart from the factor 2·5 which expresses the relative intensity of solar radiation near $H\alpha$ at the Sun's centre and limb respectively. The increase of the intensity of $H\alpha$, with increasing number of emitting hydrogen atoms within a prominence, can therefore be described by one of the familiar curves of growth which have been derived theoretically for the relation between equivalent widths of absorption lines and numbers of absorbing atoms.

Such considerations have been applied by Unsöld (*loc. cit.*) to Minnaert and Slob's observations. For a similar discussion of our own results we first confine ourselves, like

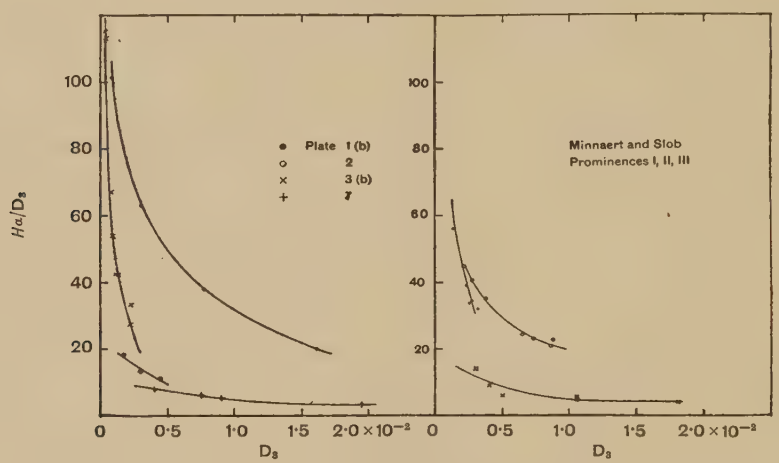

FIG. 1.—*Decrease of the Intensity Ratio of $H\alpha/D_3$ with Increasing Intensity of D_3.*

Unsöld, to the case in which the width of $H\alpha$ is solely due to Doppler broadening, the optical thickness of normal prominences being not large enough to show effects of damping. The corresponding curve of growth for a temperature of 4800° K., the temperature of the solar boundary, can then be plotted (see Fig. 2).

Equivalent widths of D_3, as can be seen from Table I, are small compared with the Doppler width of this line for a temperature of 4860° K. (=0·10 A.). Intensities of D_3 can therefore be assumed to be proportional to the number of emitting helium atoms. If the same number can also be taken as being proportional to the optical thickness of the particular prominence and region concerned, values of $\log I(H\alpha)$ in one and the same prominence when plotted against $\log I(D_3)$ should lie on curves parallel to the theoretical curve of growth for $H\alpha$. Unsöld has shown this to be true for Minnaert and Slob's prominences.

Results for our material are shown in Fig. 2 (*a*) and (*b*), where each prominence is indicated separately. For the theoretical curve of growth values of $\log (NHf/\pi W_\nu)_{H\alpha}$ are plotted against $\log I^\circ(H\alpha)/W_\lambda$ where W_λ and W_ν are the Doppler widths of $H\alpha$ corresponding to a temperature of 4800° K., expressed in wave-lengths or frequencies ($W_\lambda = 0{\cdot}33$ A.). $I^\circ(H\alpha)$ is the equivalent width of $H\alpha$ referred to the spectrum of the solar limb, or $I^\circ(H\alpha) = 2{\cdot}5\ I(H\alpha)$ where $I(H\alpha)$ is given in Table I.

For each prominence, observed values of $\log I(H\alpha)$ have been plotted against the corresponding values of $\log I(D_3)$; the resulting points have been shifted horizontally until they fall more or less on the theoretical curve. The shifts required in each case

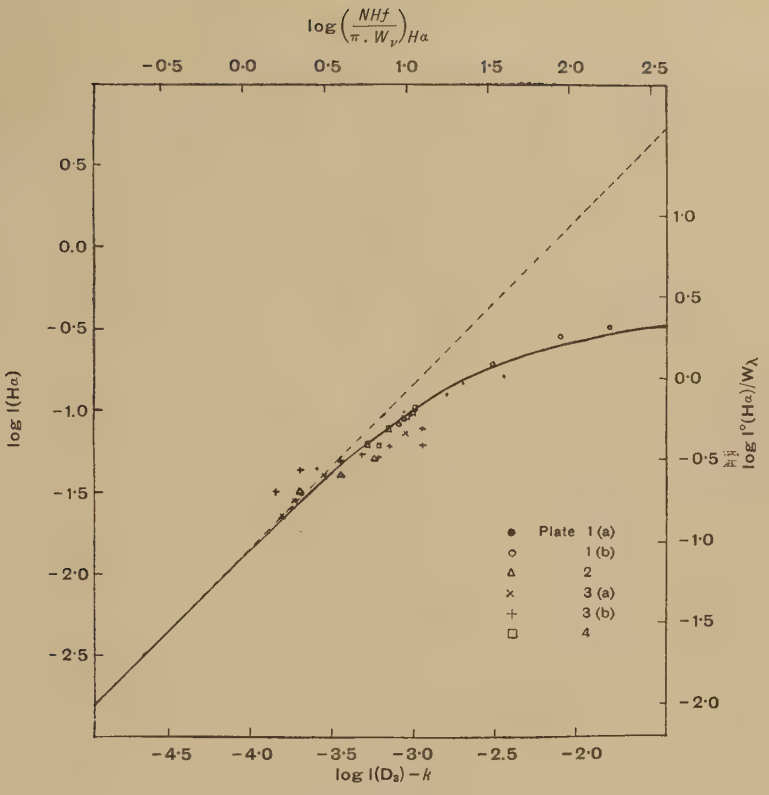

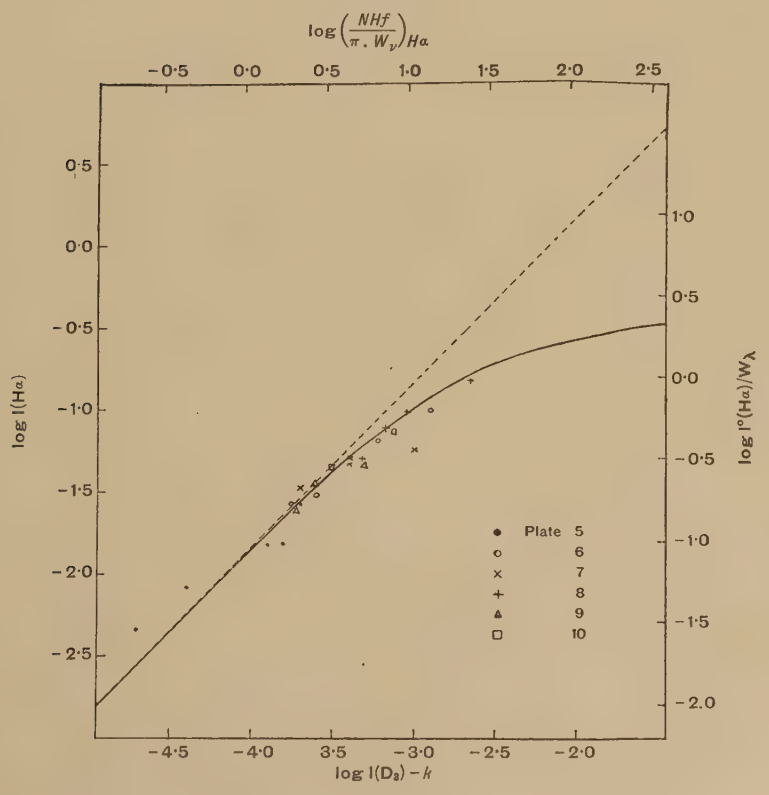

FIG. 2 (*a*) and (*b*).—*Self-absorption of Hα in Nine Prominences.*

have been given in Table I under the heading k, the abscissa in Fig. 2 being $\log I(D_3) - k$. The range covered by k for the nine prominences considered in this paper is only slightly larger than for Minnaert and Slob's observations. From what has been said earlier, it is evident that the amount of relative shifts for different prominences, or for different regions within one prominence (for the first two prominences of Table I) will give an indication of the variation of the relative numbers of hydrogen and helium atoms emitting $H\alpha$ and D_3.

With the exception of the two sets of points given by 3 (*b*) and 7, all observations agree well with the theoretical curve. This is also true for the brightest prominence investigated where $H\alpha$ appears about eight times fainter than it would be without self-absorption. It will be interesting to try to find prominences, such as chromospheric spikes, which might be still brighter in helium than those investigated here. Poor seeing conditions have made it impossible so far to photograph any low-lying regions. For very bright prominences, the effect of damping would probably have to be included together with Doppler broadening to derive the theoretical curve of growth.

If the Doppler broadening were increased, either by higher temperature than that here assumed or by turbulence, the curve would be displaced towards the straight line of slope 1 (indicated in Fig. 2), which is the limiting form of the curve of growth for infinite temperature. There is no indication that points for any of the prominences lie nearer this straight line, as they would do if there existed turbulent velocities comparable with thermal motion at 5000° K. This is true even of the first two prominences of the active type (Plates 1–3). This point is to be specially considered in our further investigations, in which distinction is made between prominences of different types, with the help of spectroheliograms. Further observations will also be needed to verify deviations from the curve of growth shown by the sets of cuts 3 (*b*) and 7 which both run in a direction rather less inclined to the horizontal axis. The same effect has been found by Unsöld for two of Minnaert and Slob's prominences; if real, it would point to a variation of k or the relative number of atoms emitting $H\alpha$ and D_3 within one and the same prominence.

Observatory,
Cambridge:
1943 *October* 1.

EXPERIMENTS TO ELUCIDATE SCATTERING IN THE SKY AND IN OPTICAL INSTRUMENTS

H. Zanstra

(Received 1943 October 1)

Summary

Scattering of light by small rock-salt crystals suspended in a saturated solution is investigated. The experimental arrangement is due to Faber, and the theoretical discussion is based on considerations by Visser. It is concluded that, for deflections below 20′ at any rate, diffraction may account for the scattering in the given suspension. For larger deflections, between 20′ and 5°, the theoretical diffraction formula is not capable of representing the observations, but there an empirical law $I \sim 1/r^{\alpha}$ holds for the scattered intensity I as a function of the distance r, with $\alpha = 2{\cdot}28$. This law is of the same type as that for the long-range scattering about a stellar image observed by Redman, but there α had the value 1·70. It is concluded that this large range scattering about stellar images may be produced by small ice crystals or perhaps other small particles in the sky. However, observations in the absence of rock salt seem to show that part of it may also be due to scattering by small particles in the instrument.

1. *Redman's Observations for Scattering in Stellar Images. Statement of the Problem. Distortion and Ordinary Scattering.*—The present paper deals with the scattering of light due to small particles and its bearing on astronomical photography.

The problem dealt with may best be introduced by considering Redman's observations for a stellar image which are contained in Table I of a paper by Redman and Shirley.* The instrument used was the 3-ft. Common reflector at the Solar Physics Observatory in Cambridge, focal length 11 ft. 4 in. In Fig. 1 of the present paper I represents the intensity measured on the photographic plate at various distances r from the centre of the image, in minutes of arc. The black dots represent Redman's observations: in Fig. 1*a*, log I is plotted against log r, in Fig. 1*b*, the same quantity is plotted against r, the logarithms being those for the base 10.

For small values of r, below 0′·1, the observations are well represented by the straight line in Fig. 1*b*:

$$\log I = 2{\cdot}14 - 14{\cdot}0\, r,$$

or

$$I = 138e^{-32{\cdot}2r} = Be^{-\beta r}, \qquad r < 0'{\cdot}1. \tag{1}$$

This type of scattering (1) may be referred to as *short-range scattering*: the intensity in the present case goes down by a factor e for an increase of 0′·031 in r and would soon become insignificant for the longer ranges.

For large values of r ($r > 0'{\cdot}5$, $\log r > -0{\cdot}3$), the observations are well represented by the straight line in Fig. 1*a*:

$$\log I = -1{\cdot}836 - 1{\cdot}70 \log r,$$

or

$$I = 1{\cdot}46 \times 10^{-2}/r^{1{\cdot}70} = A/r^{\alpha}, \qquad r > 0'{\cdot}5. \tag{2}$$

* *M.N.*, 98, 614, 1938.

This type of scattering (2) may be referred to as *long-range scattering*.

In correcting observed intensities for scattering much attention has been paid to short-range scattering of an exponential type somewhat similar to (1). Redman, however, has found that this correction is generally inadequate for large radii where the intensity drops off much more slowly, and therefore introduced what we have termed the long-range scattering.

Dr. Redman kindly permits me to quote his opinion of the two types of scattering according to his practical experience. The short-range scattering empirically represented by an exponential function of some kind is partly bound up with poor seeing and is partly of a photographic nature. In the case of a solar image the former factor generally predominates, but for stellar images taken on a fairly small scale the effect is

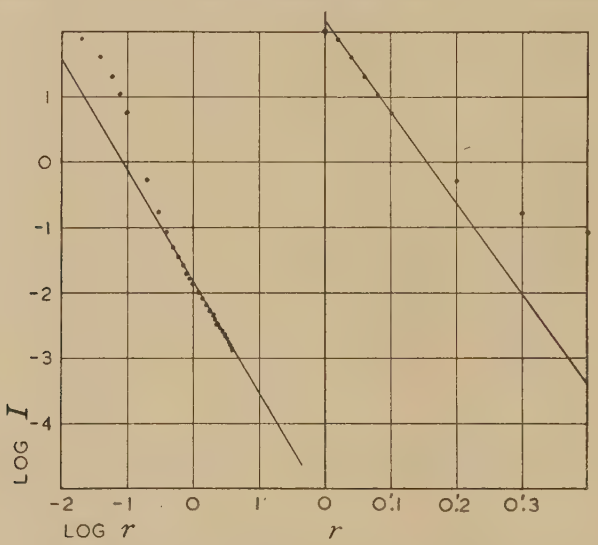

FIG. 1, *a* and *b*.—*Redman's observations of scattering about a stellar image.*

mainly photographic. The long-range scattering, on the other hand, might partly be due to scattering in the sky and partly to the instrument used.*

It is the purpose of the present paper to investigate what factors might produce a long-range scattering approximately of the type (2). The outcome of the investigation will be that small particles or small obstacles either in the sky or in the instrument may produce, for the larger radii, a scattering of approximately this type, probably by diffraction (section 4).

Anticipating this result, it may be well to point to a practical consequence. If scattering is due to small particles covering only a small portion of the background, part of the beam of light will be uninfluenced, the rest deviated, and the result is a

* Dr. Redman writes me the following particulars regarding the instrument used by him: "In the case of the Common reflector at Cambridge the scattering by the instrument may be greater than usual, because the surface of the mirror does not possess a first-class optical finish. As with so many of Common's mirrors there are numerous minute pits on the surface, due to insufficient fine grinding, and these may be responsible for some of the light observed in the outer part of the image. Also the mirror was silvered, not aluminized, and the very fine scratches always produced when polishing a chemically deposited silver coat must add to the scattered light far out in the image. Oort (*Ap. J.*, 91, 287, 1940) has confirmed the existence of 'long-range scattering' on photographs taken with the aluminized 60-inch reflector at Mount Wilson, but finds only about one-fourth the intensity measured at Cambridge for the same angular distance. The difference may also be due to the larger scale of the Mount Wilson plates, which reduces the effect of photographic scattering."

sharp image surrounded by scattered light. This kind may be called *ordinary scattering*, and the long-range scattering, if due to diffraction, is of this type. In the case of poor seeing, however, the image is either spread out or it moves about; there is no sharp image left and one has *distortion* of the image rather than scattering in the true sense. This appears to be generally true for any scattering of type (1), since there is no sharp undisturbed image.

Further, it is clear that the ranges through which each type of scattering is approximately valid should vary with the circumstances, the short-range scattering being dependent, for instance, on the seeing, and the long-range scattering on the sizes of the diffracting particles and their number.

2. *Work on Haloes and Diffraction* (*Faber*, *Visser*).—The problem under consideration is the nature of the long-range scattering about stellar images. As a first approach to this problem we shall consider some of the work done on scattering in the sky and the reproduction of similar phenomena in the laboratory.

For a general view of the phenomena in the sky and their explanation Minnaert's * book is to be strongly recommended, in particular, for our case, Chapter X on Rainbows, Haloes and Coronæ. Scattering of light in the sky is in many cases due to diffraction. In the fog bow or white rainbow the diffraction is produced by small water-drops, in the halo by small icy crystals, and in the aureole, or corona around the Moon or stars, by small water-drops, or sometimes perhaps small ice crystals.

Since both the halo and the long-range scattering of the central image are reproduced by the same laboratory experiment due to Faber, we shall in particular consider the halo. When small ice crystals of a cirro-stratus or cirrus cloud are in front of the Sun, the Sun's rays may be refracted by two faces of a crystal acting like a prism of refracting angle 60°, so that the minimum deviation for yellow light is 22°. Since the crystals have various orientations, this results in a bright ring or halo of inner radius 22°, the inner edge of which shows a succession of the spectral colours due to dispersion.† When the ice crystals become small, diffraction of light takes place resulting in coloured rings within the main ring. Visser ‡ has given an approximate theory of this phenomenon, assuming that the ice crystals act like small slits, since the exit beams have rectangular cross-sections ("We see the light source through a large number of rectangular openings: slits"). He finds agreement with an observed case for a slit width of $21 \times 10\ \mu$, which is a reasonable value for the order of the dimensions of the crystals.

Faber § has produced artificial haloes in the laboratory. Since a collection of ice crystals in air is hard to produce, he used suspensions of small crystals of various salts in their saturated solutions contained in a cell of parallel walls. Monochromatic light was used. He recognised an effect of scattering both for the direct image and the halo ring, attributing this to scattering in the cell which he did not further specify. He did not, however, carry out an actual photometry of the light scattered from the direct image.

In the present paper we shall use Faber's method for producing scattering of a central image by small crystals of rock salt, and measure the intensity of scattered light I as a function of the distance r from the centre. On the one hand this observed intensity distribution will be shown to be of the type (2) over a rather long range of r, on the other hand it will be discussed theoretically along the lines of Visser's treatment.‖

3. *Experimental Arrangement. Appearance of the Pictures. Evaluation of Observa-*

* *Light and Colour in the Open Air* (London : G. Bell & Sons, 1940).

† Another halo of radius 46° due to a refracting angle of 90° has also been observed.

‡ *Pr. R. Ac. Sc. Amst.*, 19, 1174, 1917.

§ *Kunstmatige Halo's. Waarnemingen en beschouwingen.* Doctor's Thesis, Amsterdam, 1933.

‖ When a separate name is needed for the light thus scattered about the central image, either in the laboratory or on celestial photographs, the name *aureole* seems to be appropriate. The name corona might lead to confusion in the case of the Sun.

tions.—The experimental arrangement is shown in Fig. 2 and is essentially that of Faber, except for the fact that we do not use monochromatic light. The scale of the drawing may be obtained from the height of the cell C, which was 8 cm.

A pinhole, not shown in the figure, is situated at the focus of the lens L of focal length 25·0 cm. It was illuminated by a 24-watt 6-volt lamp, 24 centimetres behind it, the filament of which was projected on it by means of a lens. The light from the pinhole is made parallel by L, and the diaphragm D cuts out a circular beam of a cross-section of one centimetre. Care was taken that the whole incident cone of light was filled. The beam now passes through a thickness of 1·5 cm. of the suspension of small rock-salt crystals contained in the cell C, and then through the objective O of the camera of focal length 17·9 cm. The front and back of the cell C consist of two plates of lantern-slide glass, 1 mm. thick, covered by two large diaphragms of diameters 2·5 and 3·7 cm. The direct beam and the scattered beams now come to a focus on the photographic plate not shown in the figure, which therefore shows an image of the pinhole surrounded by the scattered light. The diaphragm of the camera objective is opened as wide as possible, and then a beam scattered at an angle of ten degrees as indicated in the figure is still

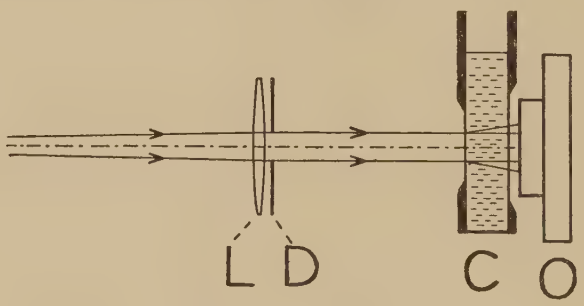

FIG. 2.—*The apparatus.*

unobstructed when passing through the compound camera lens and diaphragm. Stray light is eliminated by the two diaphragms on the cell, by a blackened perforated screen of wood on which the lens L is mounted, and by a large piece of dull black paper with a hole put in front of the pinhole. The dimensions of the plates were 8·90 × 6·35 cm., and, since the plate-holder was larger, an adapter was used.

The adjustments, made by viewing at the back of the camera, were the following: (i) The pinhole was adjusted so that its image was approximately at the centre of the plate, actually about 4 mm. above it. (ii) The diaphragm D in front of lens L was lined up centrally about the pinhole. (iii) The iris diaphragm of O was opened fully, and a piece of white paper was placed inside the cell against the front glass and illuminated by the beam. The bright spot as viewed at the back of the camera through the camera lens O was then seen to be entirely unobstructed at 3·4 cm. above and below or left and right of the image of the pinhole.

The scale of the plate was fixed by observing that 4 cm. on a scale held at the pinhole produced an image of 2·86 cm. on the ground glass at the back of the camera. To get the scale one should reckon therefore with a focal length of 25·0 cm. × (2·86/4·00) = 17·9 cm. for the camera objective, so that one degree on the plate corresponds to 0·312 cm., and the above 3·4 cm. to nearly 11 degrees for which the passage of light is unobstructed. Since the actual observations did not go beyond a radius of 7 degrees on the plate, one is sure that all of the light scattered from the primary beam fully entered the camera for each observation.

The suspension of rock salt in saturated solution was made on 1941 October 15 by dissolving the rock salt in water at 100° C. and filtering the hot solution. The filtered solution and the crystals formed in it were heated once more and evaporated at 100° C.

until the crystals began to form and then poured into a long glass bottle and cooled with water. When used on November 4 for the actual exposures it was therefore about three weeks old, so that the solution must have been well saturated. The suspension was put into the cell and stirred vigorously with a glass rod. Immediately upon this the exposure took place for the exposures of 10 seconds and longer. The shorter exposures were started 5 seconds after stirring to compensate for the fact that for the later part of the longer exposures some of the heavier crystals might have settled down.

The various exposures times were as follows:—

Na Cl exposures: 1/100, 1/30, 1/3, 1, 3, 10, 30 and 90 sec.
Sensitometer exposures: All 5 sec., a 150-watt lamp being used.

On the next day the same procedure was gone through with distilled water in the cell instead of the suspension.*

Exposures up to 1 sec. were made by means of the automatic shutter on the camera, those of 3 sec. and more, as well as the sensitometer exposures, by means of a developing clock making four ticks a second. The 90 sec. exposure was given in three portions of 30 seconds each, in between which the suspension was stirred up.

The sensitometer marks are about $1\frac{1}{2}$ cm. above and below the centre of the plate and, for exposures up to 3 sec., were impressed on the same plate, since the plate is clear at a considerable distance from the marks. For the longer exposures a separate plate with the sensitometer marks was taken and the two plates developed together. The plates used were Ilford fast U.V. Zenith Plates, $3\frac{1}{2} \times 2\frac{1}{2}$ inches, supersensitive, backed, H. & D. 700. They were developed in the dark for $3\frac{1}{4}$ min. at about 21° C. by brush development. M.Q. developer, diluted with an equal volume of water, was used, except for the 1/10 and 1/3 sec. *Na Cl* plates where pure developer for $2\frac{1}{2}$ min. was used and which were somewhat over-developed.

Before proceeding to the microphotometer tracing it may be well to consider briefly the general features of the pictures as revealed by a visual inspection of the plates.

The *Na Cl* pictures show mainly a black spot, approximately circular and fuzzed out at the other edge, as would be expected for an intensity going down with the distance from the centre. For the longer exposures, however, the outside of the spot becomes streaky, the streaks all being in the radial direction. Also one or two fairly strong extended regions of blackening appear in the upper part of the picture, probably due to reflections in the apparatus. The pictures with the water cell also show a central spot, but here, from the 1/3 sec. exposure onwards, the radial streaks become very clear and in the longer exposures are the most conspicuous feature, giving the impression that the central spot is caused by the superposition of the intersecting streaks. For these long exposures one can also see two strong reflections in the upper part of the picture and what is apparently a number of superimposed large circular regions of uniform intensity somewhat off centre, covering a big portion of the radial streak pattern. The latter might well be due to reflections in the lenses. A picture of 90 seconds exposure taken without the cell shows the same appearance, except that the two upper reflections are absent. The most likely interpretation seems to be that the two upper spots are due to reflections in the cell, the superimposed large spots to reflections at the lens surfaces, and the radial streaks to small particles or scratches in the lenses or rough edges of the diaphragms diffracting the light like small slits. The main feature in the *Na Cl* pictures, which is an intensity of radial symmetry falling off with the radius, will be interpreted in the next section as probably due to diffraction by *Na Cl* crystals acting like a very large number of small slits.

The plates taken were now run through the microphotometer of the Radcliffe Observatory. The slit of the microphotometer was adjusted to a square of 5-mm. side

* The exposures of 1/100 and 1/30 sec. for water and for *Na Cl* were made on November 6 and 7.

giving a square image of 1/6 mm. on the plate. The rate at which the paper for the tracing was run through was ten or five times that of the plate. The centre of the dark spot is entirely black and had to be located by the criterion that it is half-way between two points of equal intensity in the horizontal or vertical direction, which was done by means of the horizontal and vertical micrometer screws and readings of the deflections. Across this centre two runs were taken, a horizontal one and a vertical one, which therefore for each radius will yield four values of the intensity: left (l), right (r), down (d) and up (u). The other operations were done in the usual way, and finally, for various radii, the four values of log I for l, r, d and u could be found. It was found more con-

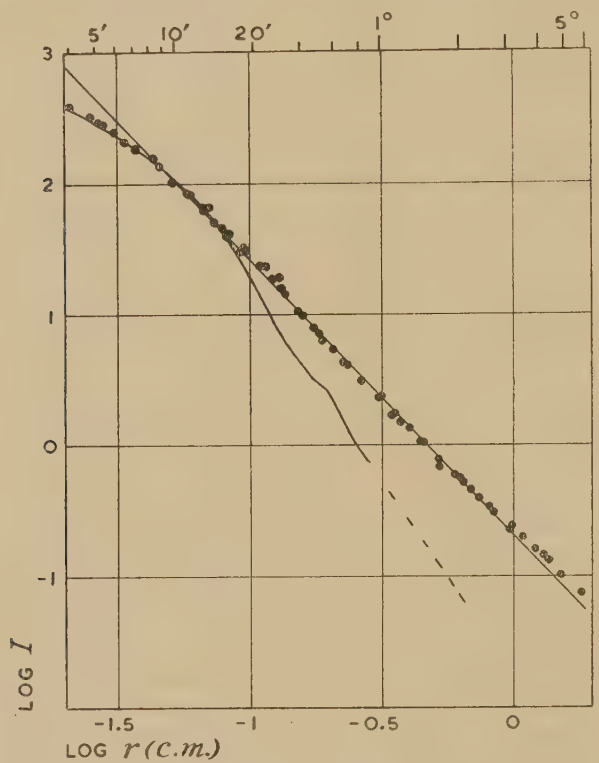

FIG. 3.—*Observations with Na Cl, uncorrected. Curve for* $W = 68\ \mu$, *straight line for* $\alpha = 2{\cdot}11$.

venient, however, to determine for one fixed log I (a horizontal line on the tracing) the four values of log r and then average them, which practically amounts to the same.

This was done for the various exposures made with *Na Cl*, and then, in the plot of log I against log r, the curves for the various exposures shifted vertically against that for the 3 seconds exposure so as to form a continuous curve. This could be done quite well, since there is a considerable overlap for the subsequent curves. The result is plotted in Fig. 3, where the black dots represent the individual observations of log I reduced to 3 seconds exposure against log r averaged for l, r, d, u.

To get the scattering due to the *Na Cl* crystals alone, the intensities of the blank experiment with water had to be subtracted. However, the two strong reflections in the upper part make any such correction in the u run illusory, and for this reason the u run was left out and the d run counted double. Thus one gets the corrected I for the *Na Cl* for each exposure separately. In most cases the intensities for water did not offer a sufficient range and had to be supplemented by shifting the log I of the next higher water exposure to the exposure in question. In the plot of log I against log r for

the various exposures the curves were then all reduced to 3 seconds exposure by vertical shift. The result is the plot of log I (corr.) against log r averaged for l, r, $2d$, contained in Fig. 4, representing the scattering by *Na Cl* crystals alone.

The water intensities by themselves were also reduced to the 3 seconds exposure by shifting, and the result is represented in Fig. 5, for the l, r, $2d$ average, which amounts to leaving out the two strong reflections above the centre.

In Fig. 6 the derivative $\alpha = -d \log I/d \log r$ is plotted against log r, with crosses for the uncorrected *Na Cl* observations and dots for the corrected ones. This derivative

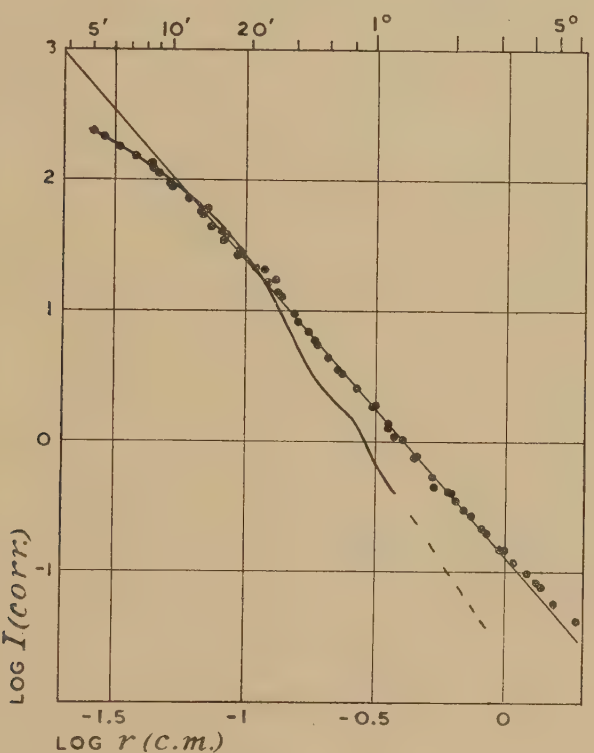

FIG. 4.—*Observations with Na Cl, corrected. Curve for* $W = 50\,\mu$, *straight line for* $\alpha = 2{\cdot}28$. *The mean values of log* r_{cm} *for the various exposures were* $-1{\cdot}42$ $(1/30^s)$, $-1{\cdot}28$ $(1/10^s)$, $-1{\cdot}12$ $(1/3^s)$, $-0{\cdot}93$ (1^s), $-0{\cdot}64$ (3^s), $-0{\cdot}42$ (10^s), $-0{\cdot}16$ (30^s), $0{\cdot}02$ (90^s).

involves no shifting of curves, except for the water corrections, and should therefore be fairly reliable.

4. *Approximate Theory and Discussion of Results. Conclusions.*—In his treatment of diffraction in haloes, Visser has made use of the fact that the faces of the crystal where the light leaves behave like rectangular windows or slits.

A similar procedure can be followed for the scattering of the incident beam. In a crystal like rock salt or ice two parallel faces behave like a plane parallel plate, so that in the absence of diffraction the light passing through them would leave as a beam parallel to the incident beam but of different phase.* When the two parallel faces are perpendicular to the incident beam, the window through which the light leaves has its

* The crystal—ice crystal in the sky or our rock-salt crystal—has dimensions of the order of one hundred wave-lengths, so that, to a first approximation, refraction and reflection occur as if the crystal were large. Also, because of the variation in size of the crystals, the light leaving may have any phase with equal probability.

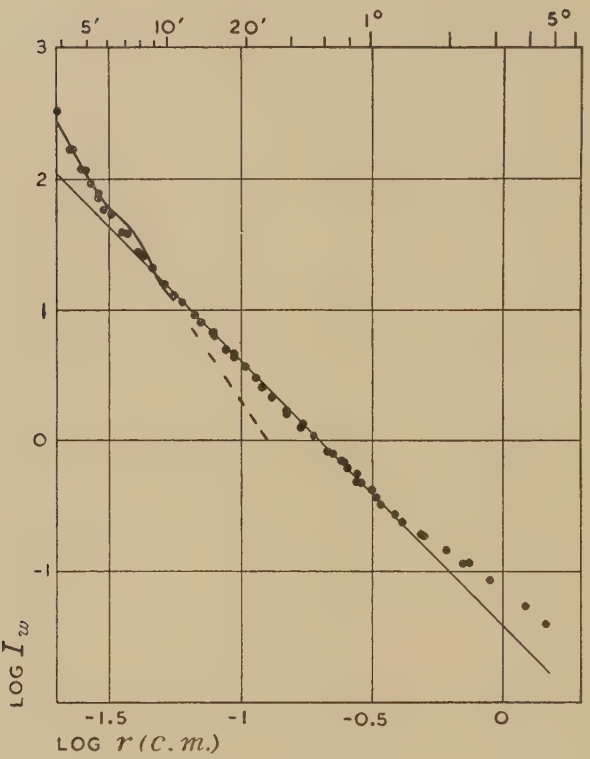

FIG. 5.—*Observations with water. Curve for $W=338\ \mu$, straight line for $\alpha=2{\cdot}03$. The mean values of log r_{cm} for the various exposures were $-1{\cdot}57$ ($1/10^8$), $-1{\cdot}46$ ($1/3^8$), $-1{\cdot}26$ (1^8), $-1{\cdot}01$ (3^8), $-0{\cdot}76$ (10^8), $-0{\cdot}49$ (30^8), $-0{\cdot}22$ (90^8).*

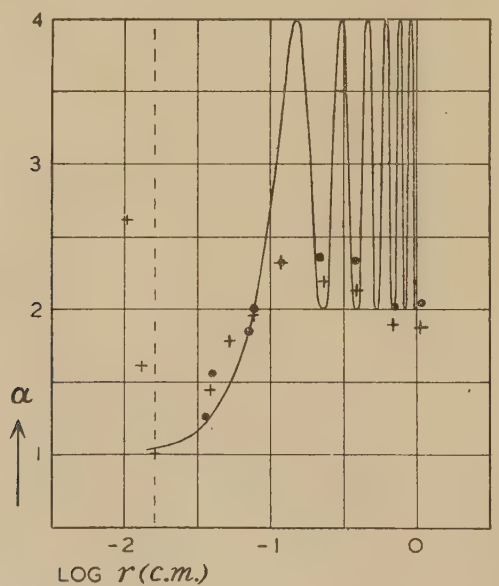

FIG. 6.—*Values of $\alpha=d$ log I/d log r. Curve for $W=50\ \mu$. Crosses for uncorrected Na Cl, dots for corrected Na Cl. Values on the left of the dotted line have no direct physical significance.*

maximum dimensions, assuming these faces to have the same shape. From this position, turning the crystal about any axis not perpendicular to the faces will make the exit window smaller, and in many cases, for instance if the axis is parallel to the faces, the window will entirely close up. So it appears that one gets a fair insight into the phenomenon if one represents the exit windows approximately by slits starting from a width zero up to a maximum, the light having arbitrary phase.

The faces of the crystal on the observer's side which do not emit but at which the light is refracted and reflected act in a similar way like dark strips of varying sizes.

The crystal as a whole may therefore be represented approximately by an area where the incident beam is intercepted and which consists of a bright slit of width w_1 where the light has arbitrary phase and an adjoining dark strip of width w_2. If the phase of the bright slit is the same as that of the incident beam, the crystal as a whole acts as a bright slit of width w_2—the width of the dark strip—on account of Babinet's principle. If the phase of the bright slit is opposite to that of the incident beam, Babinet's principle yields two adjoining bright slits. In both of them the phase is opposite to that of the incident beam, the slit w_2 having the same amplitude as the incident light and the slit w_1 having twice this amplitude. Taking the various crystals, both w_1 and w_2 vary from zero to a maximum value W of the order of the size of the crystals. It appears therefore that one can get a fair insight into the phenomenon, if one assumes that the crystals act as a number of slits of widths w varying between zero and W, though this treatment is not a rigorous one.

It can further be remarked that a slit placed in a medium, enclosed within plane parallel walls, diffracts in the same way as in air, since the portion of the medium where the light leaves the slit acts as a plane parallel plate, not influencing the directions of the beams emerging in air.

The closing-up argument does not apply to Visser's case of the halo where, near minimum deviation, the window is always the same for crystals of given dimensions. It is peculiar to the scattering about the incident beam we are dealing with.

Treating the crystals as slits of varying widths, we assume that the number of slits $n(w)dw$ having widths between w and $w+dw$ is

$$n(w)dw = Cdw, \tag{3}$$

where C is a constant and w varies from zero to W, which is of the order of the dimensions of the actual crystals.

As an approximation we shall use the formula for a slit, of which the width w is very much smaller than its length l. For a parallel beam of monochromatic light of wavelength λ incident perpendicularly, the deviation of the scattered beams takes place in a plane perpendicular to the length of the slit, and the distribution of intensity is given by *

$$I_1 = C_1 w^2 \sin^2 u/u^2, \tag{4}$$

where

$$u = \pi r_{\text{rad}} w \tag{4a}$$

and

$$C_1 = l/\lambda. \tag{4b}$$

In this expression r_{rad} is the angular deviation in radians, assumed very much smaller than unity. I_1 represents the intensity per radian, so that the total intensity is $\int_{-\infty}^{+\infty} I_1 dr_{\text{rad}}$. The constant C_1 is found by the condition that this total integrated intensity should be equal to the amount of light intercepted by the slit, which is lw, taking the

* *Cf.* R. W. Wood, *Physical Optics* (Macmillan, 1911), pp. 201, 202. Wood considers the horizontal line image formed by a lens placed behind the slit. Our case without lens follows from this by taking the focal length infinity.

incident intensity per cm.^{2} as one unit.* At the same time this verifies the occurrence of w^2 in (4). In our case the only thing that matters is that C_1 does not involve w.

For a large number of parallel slits of width distribution (3), the relative intensity resulting from (4) becomes

$$I_2=\int_{w=0}^{w=W} I_1 C dw = C_2 \frac{1}{U^2}\left\{1-\frac{\sin 2U}{2U}\right\}, \tag{5}$$

where

$$U=\pi r_{\mathrm{rad}} W/\lambda \tag{5a}$$

and

$$C_2=\tfrac{1}{2}ClW^3/\lambda. \tag{5b}$$

The actual scattering crystals are assumed to act as slits with arbitrary orientation in a plane perpendicular to the incident beam. Let there be D groups of slits (5) orientated arbitrarily, and let I represent the intensity per square radian. We then have

$$I=\frac{D}{2\pi r_{\mathrm{rad}}} I_2.$$

Substituting (5) and using (5a) and (5b), we obtain

$$I=C_3\frac{1}{U^3}\left\{1-\frac{\sin 2U}{2U}\right\}, \tag{6}$$

where

$$C_3=\tfrac{1}{4}DClW^4/\lambda^2. \tag{6a}$$

Formula (6) holds, in whatever unit I is expressed, but then C_3 depends on that unit. Differentiating (6), one obtains first

$$\frac{dI}{dU}=-4\frac{I}{U}+C_3\frac{1}{U^4}(1-\cos 2U),$$

and finally, using (5a) and (6),

$$-\alpha=\frac{d\log I}{d\log r}=\frac{r_{\mathrm{rad}}}{I}\frac{dI}{dU}\frac{dU}{dr_{\mathrm{rad}}}=-4+\frac{1-\cos 2U}{1-\sin 2U/2u} \tag{7}$$

for the slope $-\alpha$ in the $\log I$ against $\log r$ diagram. This slope is always negative, so that α is positive. For our empirical expression (2) α is a constant, but the theoretical α varies. The slope does not depend on the unit in which I or r is expressed and is the same for ordinary and natural logarithms.

In order to compare the theoretical intensities of formula (6) with the observations in Figs. 3, 4 and 5, one can evaluate I/C_3 from (6) as a function of U/π, and then plot the logarithms of these quantities against each other. We have

$$\log I=\log(I/C_3)+\log C_3, \tag{8}$$

and further, since the r in cm. is related to the r in radians by $r_{\mathrm{cm}}=fr_{\mathrm{rad}}$, where $f=17{\cdot}9$ cm., the focal length of the camera objective, we have, using (5a),

$$\log r_{\mathrm{cm}}=\log(U/\pi)+\log(\lambda f/W). \tag{9}$$

One can then try to make the theoretical curve $\log(I/C_3)$ against $\log(U/\pi)$ coincide with the plot of the observed $\log I$ against $\log r_{\mathrm{cm}}$ by a vertical shift yielding $\log C_3$ and a horizontal shift yielding $\log(\lambda f/W)$. Assuming $\lambda=0{\cdot}425\,\mu$ as a kind of average value of the wave-length of the continuous spectrum, which is approximately the photographic isophotic wave-length used for stars, one can evaluate the maximum slit width W, which

* *Cf.* M. Born, *Optik* (Springer, 1933), p. 156. One uses $\int_{-\infty}^{+\infty}(\sin u/u)^2 du=\pi$.

should be of the same order as the average dimensions of the crystals if the explanation is correct.

This shifted theoretical curve is drawn in Figs. 3, 4 and 5. One readily sees that coincidence between observation and theory can only be obtained for the smaller values of r, and this is the way in which the curves have been drawn.

The uncorrected *Na Cl* observations in Fig. 3 then yield $W=64\,\mu$, the corrected *Na Cl* observations in Fig. 4 yield $W=50\,\mu$. The actual *Na Cl* crystals were examined by making microscopic projections of two samples of the suspension and drawing the outline of the crystals. Apart from one large crystal of dimensions $300\times700\,\mu$, the largest individual crystals were about $170\,\mu$ and the smallest $30\,\mu$. The crystals had mostly collected in aggregates, rows, which were about $700\,\mu$ long and $70\,\mu$ wide, which no doubt were separated in the suspension, and so it appears that $70\,\mu$ is a reasonable value for the average size of the crystals. The agreement, as regards order of magnitude, with the theoretical value of $50\,\mu$ for W seems a convincing argument that the scattering is indeed due to diffraction by the crystals, at any rate for the smaller distances r_{cm} from the central image.

The coincidence for the smaller r's in Fig. 5 for the cell with water is not very convincing, but as far as it goes it would yield $W=338\,\mu$, indicating that the diffracting particles, which might be dust particles, scratches or bubbles in the lens system or the result of rough edges of diaphragms, are a great deal larger than the rock-salt crystals. The fact that the uncorrected *Na Cl* gives a somewhat larger W than the corrected points in the same direction.

The part of the plot for the larger r's where the diffraction formula fails can quite well be represented by a straight line in each case, of the type of the empirical formula (2) for the long-range scattering. We have

Fig. 3, *Na Cl* uncorrected, $\alpha=2{\cdot}11$,
Fig. 4, *Na Cl* corrected, $\alpha=2{\cdot}28$,

for the straight lines drawn in the figures. The accuracy of this representation is of the same order as that of the individual observations as indicated by their scatter.

In Fig. 5 for the observations with the water cell the straight line is that for $\alpha=2{\cdot}03$, but here the representation is much less accurate, as might be expected, since part of the effect is certainly due to the reflections mentioned in the previous section.*

Confining ourselves to the corrected observations for *Na Cl*, the poor agreement between theory and observation for the larger distances is quite remarkable. Formula (6) shows that for these large distances the theoretical curve should swing in small waves about the curve $I=C_3/U^3$ indicated by the broken line in Fig. 4, so that $\alpha=3$ theoretically, whereas the observed value is only 2·28.

One may think of various reasons, but none of them seems quite convincing. It may have been that there is a preponderance of very small crystals which we did not take into account theoretically, but this seems unlikely from the inspection under the microscope. The spread in λ of the light affecting the photographic plate would also tend to smooth the slopes, but this does not affect a wide range, since a factor two in λ corresponds to a factor one-half in r, or a range of only 0·30 in $\log r$.† A more weighty

* In Redman's observations of Fig. 1*a*, the straight line is that for $\alpha=1{\cdot}70$, a good deal lower than for Figs. 3, 4 and 5. It does not seem out of the question that in Redman's case we actually are still in the curved portion, and that the appearance of a straight line over a not so very large range of $\log r$ is partly accidental and partly due to superposition of the short-range scattering.

† Dr. Redman informs me that the slope of the characteristic curves for the plates used might depend somewhat on the time of exposure, that of the 30-second curve being of the order 10 per cent. greater than that of the 0·5-second curve. If a correction for an error of this kind were made, it would decrease the value of α and make the discrepancy between observation and theory larger. Moreover, the absolute value of the correction in α would probably be less than 10 per cent., since our maximum exposure is 90 sec. and our sensitometer exposure 5 sec., a factor of only 18, as compared with the above factor 60.

reason may have been the lack of stirring of the suspension for the longer exposures, where the larger crystals might have settled down. Also, though the rock-salt crystals are of the cubical type with rectangular faces, these faces often appear to be built up in steps which might lead to a preponderance of small slits. The remarkable thing in the observations, however, is not so much that the α for the larger ranges falls below 3, but that it is nearly constant for a range corresponding to a factor of 100 in r as seen from Fig. 4. The possibility should therefore be left open that either some point has been overlooked or that there is another type of long-range scattering not due to diffraction.

The conclusions drawn from Figs. 3 and 4 are further substantiated by Fig. 6, where $\alpha = -d \log I/d \log r$ is plotted against $\log r_{cm}$. The vertical dotted line indicates the size of the slit image in the microphotometer (1/6 mm.), and observations on the left of this line have no physical meaning. Besides, one gets there the short-range scattering, probably mainly photographic (section 1), which makes the α increase rapidly. The curve drawn represents the theoretical variable α from formula (7) with $W = 50\,\mu$, $\lambda = 0{\cdot}425\,\mu$. The observed α taken from the separate exposures (crosses for uncorrected, dots for corrected *Na Cl*) agrees well with the theoretical below $r = 0{\cdot}10$ cm. or 20′. Above this the observed α is practically constant, about 2·2, whereas the theoretical value oscillates rapidly between 2 and 4, corresponding in the $\log I$ plots of Figs. 3 and 4 to a wavy line about $\alpha = 3$, which is merely indicated by a broken line.

Whether the diffraction explanation holds well for all values of r, the *main conclusions* from a practical point of view seem to be the following.

The results with *Na Cl* crystals make it probable that part of the long-range scattering observed in celestial photographs arises from small ice crystals in the sky such as cause the haloes, but one may add that small particles of any kind in the atmosphere might produce a somewhat similar effect. Fig. 5, moreover, shows that another part of the long-range scattering in astronomical observations may be due to the instrument, presumably by scattering of the light by scratches, dust particles or edges of diaphragms.

For scattering by small particles like *Na Cl* crystals an empirical law of type (2) appears to hold quite well for the larger values of r. For smaller values of r—in our case below about 20′—one can change over to the theoretical law for a distribution of slit widths between zero and a maximum W, which appears to be trustworthy there. The two curves combined seem capable of representing the distribution of the scattered light with a fair degree of accuracy. Fig. 3 shows that the combined influence of scattering in the apparatus, including reflections, and scattering by small particles outside the instrument can probably be treated in the same way in many cases.

This appears to be sufficient for applying practical corrections for scattering in stellar or solar photographs, provided one can fix the value of α for the linear portion, the value of W for the non-linear portion and the value of r where the two laws join, at the same time making a correction for short-range scattering.

The work presented in this paper was carried out at the Radcliffe Observatory during the final year of the author's stay in Pretoria as a Radcliffe Travelling Fellow in Astronomy. The author expresses his sincere thanks to Dr. R. O. Redman for the generous help received from him as regards the photometry and the construction of the apparatus and for valuable discussions.

Radcliffe Observatory, Pretoria,
and Howard College, Durban:
1943 *July.*

THE VARIATION OF LATITUDE AT GREENWICH, 1936–40

(Communicated by the Astronomer Royal)

(Received 1943 September 4)

Summary

The observations with the Cookson floating zenith telescope, made at the Royal Observatory, Greenwich, from the introduction of the new programme of observations in 1936 to the termination of observations in 1940, have been reduced and discussed. The variation of latitude at Greenwich during this period has been determined.

---

1. Preliminary values of the latitude variation at the Royal Observatory, Greenwich, for the years 1936–38, based on observations with the Cookson floating zenith telescope, have been given by H. R. Hulme.* A new star-programme had been introduced in 1936, when the instrument was moved from the courtyard of the Royal Observatory to a site in the Christie Enclosure, adjacent to the reversible transit instrument. In the new programme, consisting of 24 groups of pairs of stars, each group extending over approximately one hour of R.A., three groups are observed nightly, centred at Greenwich mean midnight. Thus each group can be directly connected with groups on either side of it differing by, at most, 2^h in R.A., and the group connections are not so strongly determined as in the previous programme, in which evening and morning observations were obtained. For this reason and because also of the paucity of material available, the group corrections derived by Hulme were extremely weak.

2. Observations were continued until the autumn of 1940, when they were interrupted by the nightly air-raids on London. The instrument received slight damage, and the objective and telescope were dismounted and stored away for safety. The resumption of observations is not at present possible; if observations are resumed on the same site and with the same general programme, the effects of precession will necessitate changes of star-pairs in several of the groups. It seemed desirable, therefore, to use the available material to derive stronger group corrections and to determine the variation of latitude for the four years over which the observations extended.

3. Using preliminary star-places, based in general on the Albany *General Catalogue*, the mean differences between the several star-pairs forming one group were determined and corrections were derived to reduce each pair to the mean of the group. These corrections were applied and the group means for each night of observation were formed. The differences between the groups were then subjected to a process of adjustment. Considering, for instance, groups I to IV, there is direct connection between two adjacent groups, I and II, II and III, III and IV, in two consecutive periods of observation; there is also direct connection between I and III, and between II and IV, in one period of observation. There are thus five equations from which, by a simple process of adjustment, the three differences (I–II), (II–III), (III–IV) can be derived. Similar adjustments were made for groups II to V, III to VI and so on. Thus, finally, three separate determinations of each of the consecutive group differences were derived, which were not, however, entirely independent. The arithmetic mean of these were taken as provisional group corrections. These provisional values were good enough for combining groups observed on the same night but the amount of material available was not sufficient for the accurate control of the general system of the star-places. Thus, for example, comparison between groups I and XII would involve the summation of the differences (I–II), (II–III), . . ., (XI–XII), with corresponding accumulation of

* *M.N.*, 99, 202, 1939.

error. The general system of the star-places was therefore controlled in two ways: (*a*) The system of declinations of the *General Catalogue* is known to require a correction depending upon R.A. which, for the declination of the zenith at Greenwich, was investigated by Hulme.* The group corrections for the 24 Cookson groups should closely reproduce this periodic correction depending upon R.A.; (*b*) the International Latitude Service has published values of the latitude variation up to 1939·0 and, though the values of the x component are not necessarily applicable directly to Greenwich, they serve to provide an indirect control. The two methods of controlling the general system of star-places proved to be in close agreement.

4. The finally adopted group corrections are as follows:—

Group Corrections

(To be added to Observed – Tabular Z.D. north)

Group	Correction	Group	Correction	Group	Correction	Group	Correction
	″		″		″		″
I	+·021	VII	+·318	XIII	−·077	XIX	−·121
II	+·288	VIII	+·180	XIV	−·055	XX	−·040
III	+·087	IX	−·036	XV	+·052	XXI	−·194
IV	−·035	X	−·095	XVI	−·054	XXII	−·017
V	+·048	XI	+·038	XVII	−·098	XXIII	−·153
VI	+·211	XII	−·065	XVIII	−·096	XXIV	−·118

These corrections contain the periodic term in R.A.

$$+0''\cdot118 \sin \alpha + ''0\cdot012 \cos \alpha.$$

Thus corrections of these amounts require to be added to the tabular Z.D.'s or to the tabular declinations to give the observed values. These corrections are in close agreement with those found by Hulme.

5. The mean values of the latitude variation for each period of observation were derived. These were combined into two series of overlapping means, each of approximately equal weight, averaging 25 plates, plotted, and a smooth curve was drawn through them. From this curve the following values of the latitude variation, applicable to observed N.P.D.'s, were read off:—

Variation of Latitude at Greenwich

(Applicable to N.P.D.)

Year / Fraction of Year	1936	1937	1938	1939	1940
	″	″	″	″	″
0·0	...	+·02	+·10	+·10	+·17
·1	...	+·04	+·13	+·13	+·20
·2	...	+·04	+·11	+·10	+·13
·3	...	+·03	+·04	+·05	+·04
·4	...	+·01	−·03	−·01	−·04
·5	...	−·03	−·12	−·07	−·10
·6	−·11	−·08	−·17	−·13	−·14
·7	−·06	−·11	−·13	−·14	...
·8	−·03	−·03	−·05	−·09	...
·9	·00	+·05	+·03	+·03	...
1·0	+·02	+·10	+·10	+·17	...

* *M.N.*, 99, 199, 1939.

Erratum

M.N., **103**, No. 4, E. H. Linfoot's paper:

Page 210, footnote †, *for* the angular deviation which it imparts to the rays, *read* the retardation which it imparts to the wave-fronts.